THE CATHOLIC UNIVERSITY OF EASTERN AFRICA

(CUEA)

FACULTY OF SCIENCE

DEPARTMENT OF MATHEMATICS AND COMPUTER SCIENCE

MATHEMATICAL MODELING OF INFECTIOUS DISEASE POPULATION DYNAMICS: A STUDY OF MEASLES IN NIGERIA

MATE OLUGBENGA PHILIP, *fms*

MSc/M/1018626

A RESEARCH PROJECT SUBMITTED IN PARTIAL FULFILMENT OF THE REQUIREMENTS FOR THE AWARD OF A MASTER OF SCIENCE DEGREE IN APPLIED MATHEMATICS

2013

DECLARATION

This research project is my original work. It has not been submitted to any university or institution for an award of a degree.

Signed _____ Date _____

MATE Olugbenga Philip, *fms*

MSc/M/1018626

This research project has been submitted with our approval as University Supervisors.

Signed _____ Date _____

DR. MARK KIMATHI

Signed _____ Date _____

DR. BETWELL OWUOR

DEDICATION

This research project is dedicated to

Akanbi and ***Abosede***

And

My bi-faceted family

ACKNOWLEDGEMENT

I am grateful to the Creator and Sustainer of the created cosmos – my fount and end.

I am grateful to The Catholic University of Eastern Africa for accepting me to explore the world of graduate studies under her tutelage and to my lecturers for sharing with me from their wealth of knowledge and expertise as they know best and/or deemed best.

My supervisors Dr. Mark Kimathi and Dr. Betwell Owuor were good guides to me as I negotiated the murky waters of my project. Thank you for your availability and dedication.

Dr. Sikiru Olanrewaju Badaru of the Epidemiology Division, Nigeria Center for Disease Control, Federal Ministry of Health, Abuja facilitated my access to the weekly Nigeria measles data for 2012. I am grateful for your unquantifiable assistance.

I am grateful to the members of my bi-faceted family, friends and people of good-will whose divergent support sustained and enabled me to bring this phase of my study to a convergent end.

I am especially grateful to Joachim Ezetulugo - Okoye, *fms* who initiated this phase of my study. Thank you for the opportunity.

NOMENCLATURE

$S(t)$	The number of susceptible individuals at time *t*
$E(t)$	The number of exposed individuals at time *t*
$I(t)$	The number of infective individuals at time *t*
$R(t)$	The number of recovered individuals at time *t*
I_0	Initial value of the infective class
S_0	Initial value of the susceptible class
$I_{\max}$	The maximum (possible) number of the infective class
S_∞	The number of susceptible individuals after the epidemic
N	The total size of the population
r	The rate of infection of the susceptible class per unit time
β	The rate of infection of the susceptible class per unit time
a	The rate of removal of the infective class per unit time
λ	The rate at which the exposed become infective per unit time
R_0	The basic reproduction number
R	The replacement number
σ	The contact number
μ	The death rate. μ^{-1} is life expectancy
$\mathbb{R}^2$	2-dimensional Euclidean space
L	Average life expectancy

ABSTRACT

This study employed the SIR and SEIR models to mathematically study and describe the epidemiology of measles in six states representing each of the geo-political zones of Nigeria.

A dynamical system's long term behavior is of paramount biological importance. This behavior is known through the mechanism of stability analysis. This work established the necessary condition for the system to be stable.

Qualitative analysis allowed the exploration of the dynamics of the disease without solving the systems. Important parameters with threshold values helped determine under what condition an epidemic is possible. For a wholly susceptible population, this parameter is the basic reproduction number while the replacement number is the threshold parameter for a population that is not wholly susceptible.

Numerical simulations were done using *MatLab* 7.10.0.499 (R2010a) while *Math Type 6.9* was used for writing the equations. The data used was obtained from the Surveillance Branch, Epidemiology Division, Nigeria Center for Disease Control, Federal Ministry of Health, Abuja.

Although basic, the SIR model is insightful into the mechanism of measles vis-à-vis the constituting compartments but handicapped in adequately describing the incidence of measles in the regions studied. A closer representation of the biology of the disease vis-à-vis its evolution is captured by the SEIR model. Although, it is an improvement of the SIR model, without vital dynamics, it is inadequate in describing the measles incidence of the regions. However, the model with vital dynamics rescued the cyclic repetition observed in time series plot of measles incidence. Consequently, it is the model that is closest to the reality of the incidence data in spite of its inability to sustain the observed oscillations.

Table of contents

1.0 CHAPTER ONE

1.1 INTRODUCTION

Measles is an infectious (contagious) disease of the respiratory system. The virus causing measles belongs to the *Paramyxoviridae* family and genus *Morbilivirus.* This virus lives in the mucus in the nose and throat. According to the Centre for Disease Control (CDC), when an infected person sneezes or coughs, fluid droplets spray into the air. These droplets can get into other people's noses or throats when they breathe or put their fingers in the mouth or nose after touching an infected surface. Measles is particularly a human disease as it is not known to have an animal reservoir (Bradsher et al, 2006; WHO [42]).

Measles is characterized by fever which reaches its maximum on the fourth day, cough, sneezing, running nose, conjunctivitis (red itchy eye), Koplik's spots (tiny white lesions on the inside of the cheek) and the measles rash which begins on the back of the ears before spreading to cover most of the body. The measles bulletin as reported by Bradsher et al (2006) posit that 40% of the 3 million deaths among children each year is attributable to this vaccine preventable disease while the World Health Organization [42] reports that there were 158,000 measles deaths (mostly children) globally in 2011. This translates to about 430 deaths every day or 18 deaths every hour.

Over the past one hundred years, mathematics has been used to understand and predict the spread of diseases, relating important public health questions to basic transmission parameters (Bakare et al 2012). Although the dynamics of disease appear to be very complex as observed by Lewis (2004), simple mathematical models can be used to understand features governing the outbreak

and persistence of an infectious disease as it provides a framework for data analysis and interpretation (See McLean and Anderson, 1988).

Hethcote (2005) observed that in our days, any work related to an illness needs the use of mathematical models. Hinged on the advantage of mathematical models is that the results can be evaluated and compared to known data. This affords the opportunity to identify a model's strength and weakness.

Given the above observation by Hethcote, this study focused on the study of the Kermack - Mckendrick SIR (Murray, 2002) model and the SEIR (Anderson and May, 1982; Trottier and Philippe, 2002) epidemiology models. The SIR model is a Susceptible-Infective-Removed (SIR) compartmental model. It assumes that a population can be divided into three mutually exclusive classes. Those who are vulnerable to the disease are in the susceptible class, those who can transmit the disease to others are in the infective class while those who are immune are in the recovered class (Glenn, 2005). The SEIR model, unlike the SIR has an extra compartment for those who have the virus but cannot yet transmit the disease to others. The SEIR model is considered with and without vital dynamics.

A more detailed model will be a better description of a specific disease. It will however require more parameters. Given that data are often inaccurate and incomplete due to underreporting and misdiagnosis, a simple model may give better predictions (Brauer, 2004). It is to this end that the SIR and SEIR models were considered.

This study explored the dynamics of an infectious disease as captured by the SIR and SEIR epidemiology models and then applied it to the available measles data of Nigeria.

1.2 WHY EPIDEMIOLOGICAL MODELING?

According to the Encyclopedia and Dictionary of Medicine, Nursing and Allied Health, epidemiology is "the science concerned with the study of the factors determining and influencing the frequency and distribution of disease, injury and other health-related events and their causes in a defined population for the purpose of establishing programs to prevent and control their development and spread". Given that measles is conventionally thought of as belonging to the exclusive domain of medicine because it is a disease, why would mathematics attempt to usurp this established medical province?

There is a sense in which Mathematical modeling can be described as the link that connects mathematics to other disciplines. Focusing on diseases and borrowing from Hethcote (2005), mathematical modeling has significant and profound contributions to make to the study and understanding of infectious diseases. These include but are not limited to:

- Mathematical modeling allows an exploration of the effects of different assumptions and formulations
- The model's behavior can be analyzed using mathematical methods and computer simulations
- It can be used to compare diseases of different types or at different times or in different populations
- Mathematical modeling is useful for theoretical evaluation, comparison and optimization of detection, prevention and control programs
- It can be used to identify trends, and to make forecasts
- Results can be evaluated and compared to empirical data. This helps identify a model's strength and weakness

- Models can also be extremely useful in giving reasoned estimates for the level of vaccination for the control of directly transmitted infectious diseases (Murray, 2002).

For an in-depth discussion of the importance of mathematical epidemiological modeling, see Hethcote (2005).

1.3 MEASLES TREND IN NIGERIA (1980 – 2011)

The country experienced measles incidence in excess of 115,000 per annum in the first 7 years culminating in 1986 with a high of 182591 in 1984. A marked reduction followed with an upsurge every four years in excess of 106000.

According to the WHO key facts [42], measles vaccination resulted in 71% drop in measles death between 2000 and 2011 worldwide. The corollary of the vaccination is that the incidence of the disease will decrease. However, it is to be noted that a significant effect of this vaccination efforts would only be felt from 2006 onwards with an all-time low of 704 in 2006 and a high of 18843 in 2011 which is relatively insignificant when compared with the 1980 – 1986 period. It can thus be said that measles is currently endemic (always present) in Nigeria.

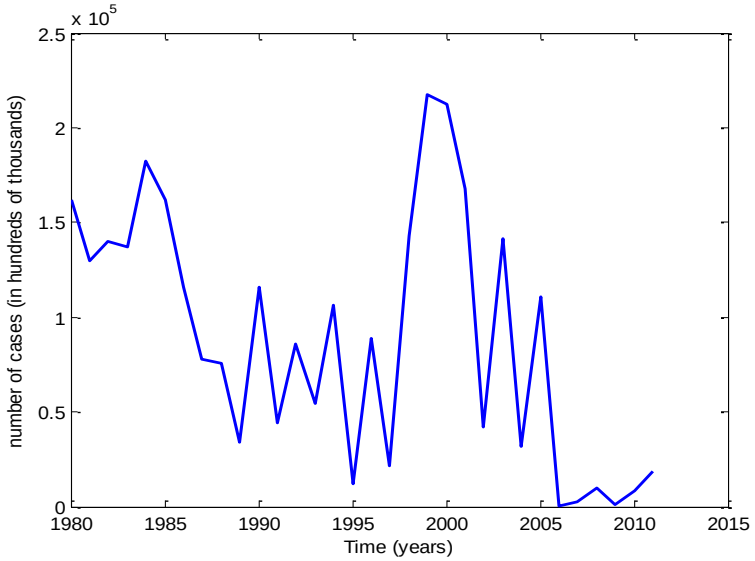

Figure 1.1 Measles trend in Nigeria (1980 - 2011). The data is available at http://www.who.int/entity/immunization_monitoring/data/incidence_series.xls

1.4 LITERATURE REVIEW

One of the earliest written descriptions of measles as a disease according to the CDC was provided by Rhazes - a Persian physician in the 10th century. He described the disease as "more dreaded than smallpox". According to the CDC, and Axton (1979), Francis Home, a Scottish physician demonstrated in 1757 that measles was caused by an infectious agent present in the blood of patients while Enders and Peebles isolated the virus that causes measles in 1954 at Boston, Massachusetts.

Murray (2002) used the SIR model on the 1978 influenza epidemic in an English boarding school reported in the British medical journal, *The Lancet*. A best fit numerical technique was used directly on the equations of the system for comparison with the available data. Though Murray did not give an indication as to how the parameters were estimated, he concluded that the epidemic was severe since R/σ is not small. Keeling and Rohani (2008) however used the least squares procedure to estimate the parameters from the data and concluded that the model dynamics with the estimated parameters was in good agreement with the data.

Raggett (1982) applied the SIR model and a comparative stochastic model to the 1665 – 1666 outbreak of plague in the village of Eyam in England. Murray(2002), in reporting him, made the case that the comparison between the solutions from the deterministic model and the Eyam data was very good as it was better compared to the result obtained from the comparative stochastic model. The work showed how to determine the parameters from the available data and knowledge of the etiology of the disease.

Hirst et al (1977) constructed an engineering-economic model to simulate energy use on an annual national basis from 1970 to 2000. The aim was to provide an analytical tool that enables an evaluation of a variety of energy conservation policies and technological improvements vis-à-vis how they impact on residential energy use and expenditures over time. The study concluded that the model developed performed very well given the model's outputs with historical data for 1960 – 1974 and with other forecasts to 2000.

Hethcote (2005), Asor and Ugwu (2011) credited Daniel Bernoulli, a physician with the earliest account of mathematical modeling of the spread of disease. Bernoulli formulated and solved a model for smallpox so as to evaluate the effectiveness of inoculation with the smallpox virus. According to Asor and Ugwu, Bernoulli's study showed that inoculation against smallpox would increase the life expectancy from 26 years 7 months to 29 years 9 months.

That deterministic epidemiology modeling seems to have started in the 20th century finds an echo in Hethcote (2005). He gave the example of Hamer who formulated and analyzed a discrete time model in 1906 in an attempt to understand the recurrence of measles epidemics and Ross who interested in the incidence and control of malaria, developed differential equations model for malaria as a host-vector disease in 1911.

Scholars of Mathematical Modeling (Murray, 2002; Brauer, 2004; Hethcote, 2005) affirm the work of Kermack and McKendrick on epidemic models and the major influence it had on the development of epidemiological modeling scholarship. The classic SIR model owes its existence to Kermack and McKendrick.

A modified SIR model was used to simulate infectious disease dynamics in Rivers State, Nigeria over a ten year period (2000 – 2009). This study, using a comprehensive epidemiological data

from the Federal Ministry of Health, analyzed the model and concluded that equilibrium analysis helps to investigate whether disease spread could attain pandemic level or it could be wiped out (Asor and Ugwu, 2011). It is to be noted that the nature of the infectious disease(s) investigated was not explicitly given.

Bakare et al (2012) used a deterministic, compartmental SEIR model to simulate the dynamics of the transmission of measles on a variable size population that is homogeneously mixing. The study addressed the stability of the disease-free and endemic equilibrium and carried out numerical simulation.

Tuberculosis disease population dynamics was simulated based on the standard theory of SIR by Koriko O. and Yusuf T.T (2008). The work showed the disease free equilibrium to be stable while the stability of the endemic equilibrium is a function of the model parameter values.

Apostolou Maria (2011) used the deterministic SIR and SEIR models with both constant and variable contact rate to simulate the dynamics of measles. Her comparative study focused on New York, Portsmouth and London. The simulation for New York compared well to the data while those for Portsmouth and London were not as good.

Macdonald et al (2012) studied disease spread over a network using the SIR model. The study showed that the ability of a centrality measure to identify spreaders can be sensitive to the β parameter and that given a β value above the epidemic threshold, eigenvector centrality performs very well.

The A/H1N1 – 2009 virus pandemic was studied by Rodriguez-Meza (2012) using the SIR model and the available data for Mexico. The study showed that the parameters used are in

agreement with the ones obtained by fitting the Mexican data. Consequently, the study made predictions about the spatial and temporal behavior of the epidemic

It is to be noted that this review of literature is not an exhaustive and definitive rendition of scholarship on epidemiology modeling given that the literature is extensive and growing steadily.

1.5 STATEMENT OF THE PROBLEM

On the one hand, although global incidence has been significantly reduced through vaccination, measles remains an important public health problem while on the other hand, the persistence of measles in many African countries points to the need to further investigate the dynamics of the disease epidemics in endemic areas (Grais et al, 2006).

1.6 OBJECTIVES OF THE STUDY

1. To analyze the Kermack-McKendrick model
2. To describe measles dynamics (the evolution of measles with time) with the SIR and SEIR (with and without vital dynamics) models and examine the extent to which they describe the incident of measles as represented by the epidemiology data for the regions.
3. To examine the long-term behaviour of the solutions
4. To compare the numerical simulations of the models

1.7 SIGNIFICANCE OF THE STUDY

1. It will add to the available literature in helping to understand the dynamics of measles
2. Public health policy decision makers will have a tool for the evaluation of the effectiveness of control measures in the country

1.8 LIMITATIONS OF THE STUDY

1. According to WHO, disease incidence data usually represent only a fraction of the cases. This means that data are often incomplete and inaccurate because of under-reporting and misdiagnosis (Brauer, 2004). However, the collected data are useful in monitoring trends.
2. It is to be noted that an epidemiological model is a simplification of reality.
3. The absence of age-dependent population in the models as would be expected of measles is consequent on the lack of specific age-stratified data.
4. The assumption of a homogenously mixing population

2.0 CHAPTER TWO

This chapter presents the SIR and the SEIR models to be studied.

2.1 THE KERMACK-MCKENDRICK MODEL

The Kermack-McKendrick model (Murray, 2002) is a compartmental model with three basic classes. These are:

- Susceptible (S)
- Infective (I)
- Removed (R)

As the schematic diagram below shows, this model is formulated in terms of the rates of flow of members of the population between compartments. There is a flow from S to I representing the rate of new infections and a flow out of I representing the rate of recovery. Mathematically, these rates of change are described as derivatives with respect to time t (Brauer, 2004). The right hand side of equation (1.1) gives the evolution rules for each compartment.

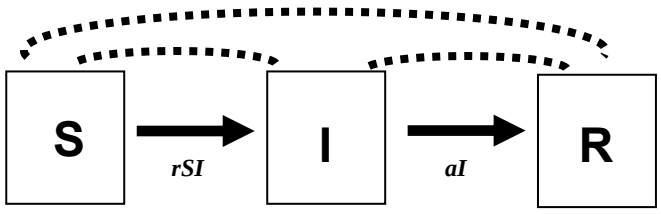

Figure 0.1 A schematic diagram of the SIR model. The boxes give compartments. The arrows indicate the disease progression while the dotted lines indicate the interaction between the different compartments.

The susceptible are lost at a rate proportional to the number of Infective and Susceptible, rSI where $r > 0$ is the rate of infection. The gain in the infective class is also at this rate while the rate at which the infective are lost to the Recovered class is aI where $a > 0$ gives the removal rate of infective.

Hence the model is

$$\begin{aligned} \frac{dS}{dt} &= -rSI \\ \frac{dI}{dt} &= rSI - aI \\ \frac{dR}{dt} &= aI \end{aligned} \tag{1.1}$$

with initial conditions $S(0) = S_0 > 0, \quad I(0) = I_0 > 0, \quad R(0) = 0$ (1.2)

The constant population size is built into the system. Adding the equations making up the system (1.1) yields $\frac{dS}{dt} + \frac{dI}{dt} + \frac{dR}{dt} = 0$

$$\Rightarrow \qquad S(t) + I(t) + R(t) = N \tag{1.3}$$

Thus, upon determining $S(t)$ and $I(t)$, $R(t)$ can be determined as $R(t) = N - S(t) - I(t)$

We can then consider the coupled system

$$\begin{aligned} \frac{dS}{dt} &= -rSI \\ \frac{dI}{dt} &= rSI - aI \end{aligned} \tag{1.4}$$

With initial conditions $S(0) = S_0 > 0, \quad I(0) = I_0 > 0$ (1.5)

According to the initial conditions:

- The number of Susceptible at time $t = 0$ is greater than zero. If otherwise, the disease cannot spread as there is no population to be infected.
- The number of Infective at time $t = 0$ is greater than zero. If it were zero, the disease is absent in the population and consequently there won't be any dynamics to study.
- The number of Recovered is zero. At this initial time, no member of the population has recovered from the disease which is yet to be transmitted.

2.2 ASSUMPTIONS OF THE MODEL

The assumptions upon which this model is based are:

i. The population size N is constant

ii. The population consists of susceptible, infective and the removed.

iii. The incubation period of the disease is short enough to be negligible. An individual who contracts the disease becomes infective immediately. This translates to zero latent period.

iv. The population is uniformly mixing

v. The infection rate is constant and the infective recovers at a constant rate

vi. After recovery, lifelong immunity is conferred.

2.3 THE SEIR MODELS

The SEIR model is a compartmental model with four basic classes. These are:

- Susceptible (S)
- Exposed (E)
- Infective (I)
- Removed (R)

The flow pattern of this model is similar to that of the SIR described earlier say for an additional compartment (Exposed) between the Susceptible and the Infective compartments. For this model, the Susceptible who contracts the virus progresses to the Exposed compartment. The exposed, though having the virus cannot infect until after a given latent period when they become infective. The period between the time of exposure and the onset of infectiousness is the latent period. The SEIR model better captures the biology of measles than the SIR model. Two types of this model are considered in this study: the model without vital dynamics (no birth and death) and with vital dynamics (birth and death).

The constants r and a in equations (1.6) and (1.7) are equivalent to r and a of the SIR model and are defined as such, $\lambda > 0$ is the rate at which the exposed become infected and $\mu > 0$ is the death rate.

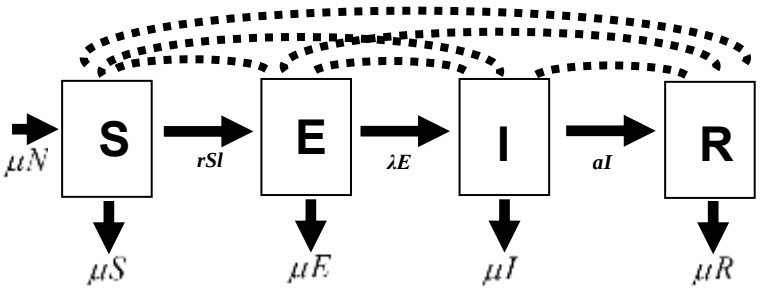

Figure 0.2 A schematic diagram of the SEIR Model. The boxes give compartments. The arrows indicate progression of compartment members while the dotted lines indicate the interaction between the different compartments. μ is equal to zero for the model without vital dynamics.

The model without vital dynamics (Trottier and Philippe, 2002) is

$$\begin{aligned} \frac{dS}{dt} &= -rSI \\ \frac{dE}{dt} &= rSI - \lambda E \\ \frac{dI}{dt} &= \lambda E - aI \\ \frac{dR}{dt} &= aI \end{aligned} \tag{1.6}$$

The model with vital dynamics (Anderson and May, 1982) is

$$\begin{aligned} \frac{dS}{dt} &= \mu N - \mu S - rSI \\ \frac{dE}{dt} &= rSI - (\mu + \lambda) E \\ \frac{dI}{dt} &= \lambda E - (\mu + a) I \\ \frac{dR}{dt} &= aI - \mu R \end{aligned} \tag{1.7}$$

With initial conditions $S(0) = S_0 > 0,\ E(0) = E_0 > 0,\ I(0) = I_0 > 0,\ R(0) = 0$ (1.8)

The notations for the SEIR model with and without vital dynamics were modified from the one in the original paper to suit the nomenclature adopted for this study.

2.4 ASSUMPTIONS OF THE SEIR MODELS

i. The population size N is constant. For the model with vital dynamics, the net input by births is equal to the net mortality.

ii. The population consists of susceptible, exposed, infective and the removed.

iii. The population is uniformly mixing

iv. The parameters a, r and λ are constants

v. After recovery, lifelong immunity is conferred.

3.0 CHAPTER THREE

3.1 INTRODUCTION

If a small group of infected individuals $I_0 > 0$ is introduced into the population of $S_{0,}$ will the infection spread or not assuming we know *r* and *a*? In other words, will there be an epidemic? The domain of interest is in the infection spreading. Hence the task at hand is to describe how the infection will spread with time in the population. Will the number of those infected increase continuously with time? At what rate will this increment be? If it will not increase continuously with time, when will it begin to decline? What is responsible for this decline? And to what extent will it decline? Will every member of the population contract the disease?

3.2 QUALITATIVE ANALYSIS

This is a tool that helps to visually establish the long term behavior of the trajectories (solution curves) and its interplay with the model's parameter value(s). In studying dynamical systems, the use of phase portrait offers an invaluable tool in understanding the system's dynamics without actually solving the associated Differential Equations. Braeur (2006) demonstrated that general epidemic models (the SEIR inclusive) have the same asymptotic behaviour as the SIR model. Hence, it suffices to examine the SIR model qualitatively without loss of generalization.

Theorem 1: (Existence and Uniqueness of Trajectories)

Consider an autonomous system of differential equations in $\mathbb{R}^2$

$$\frac{dx}{dt} = f(x, y) \ , \ \frac{dy}{dt} = g(x, y) \tag{1.9}$$

with initial conditions $\mathrm{x}(0) = x_0 \ , \ \mathrm{y}(0) = y_0$ (1.10)

If the functions $f(x,y)$ and $g(x,y)$ have continuous first derivatives with respect to both x and y on a region say *R* in the xy-plane, then, the autonomous system (1.9) has exactly one trajectory through each point $(x_{0,}y_o)$ in the interior of R.

This theorem implies that geometrically, only one trajectory can pass through a point. Consequently, trajectories cannot cross each other.

3.2.1 EQUILIBRIUM POINT(S)

The **critical** or **equilibrium** point(s) for (1.9) is a solution of the algebraic equations

$$f(x,y)=0, \quad g(x,y)=0 \tag{1.11}$$

If x^* and y^* be the solutions of(1.11), then we have $x(t)=x^*$ and $y(t)=y^*$ as constant solutions of(1.9). The constant solutions are called equilibrium solutions or fixed points and they represent degenerate trajectory (they do not evolve as *t* increases). Equilibrium points represent the points for which the variables do not change with time.

Thus, using(1.4) and (1.11) yields

$$\begin{aligned} -rS^*I^* &= 0 \\ rS^*I^* - aI^* &= 0 \end{aligned} \tag{1.12}$$

which upon simplifying yields $I^*=0, \quad S^*\geq 0$ (1.13)

Thus, the line $I=0$ (positive S-axis) represents the domain of the equilibrium points for the system. Negative numbers are not considered for population.

3.2.2 NULL CLINE

A curve in the phase plane on which the direction of evolution of solution curves all point in a direction parallel to a coordinate axis defines a **null cline.** Null clines are isoclines with $g(x,y)=0$, whose path cuts the vertical axis with zero slope and $f(x,y)=0$ whose path cuts the horizontal axis with infinite slope.

For the S (horizontal axis) null cline

$$f(x,y)=0 \quad \Rightarrow \quad -rSI=0 \tag{1.14}$$

So that $S=0,\ \ I=0$ are solutions since $r>0$

For the I (vertical axis) null cline

$$g(x,y)=0 \quad \Rightarrow \quad (rS-a)I=0 \tag{1.15}$$

So that $S=\frac{a}{r},\ I=0$ are solutions since $r>0$

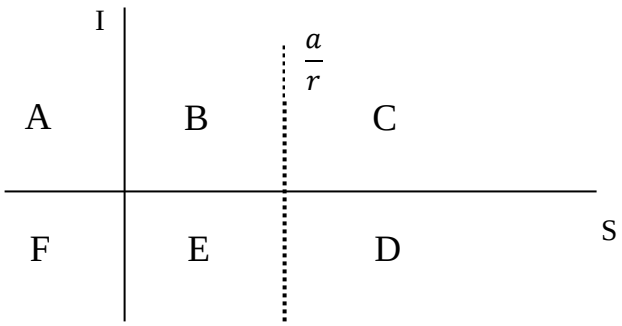

Figure 3.1 The S and I null clines.

The use of equation (1.4) enables us to determine whether S and I are decreasing or increasing in each section of the figure above. Along the I axis, $\frac{dI}{dt}=-aI, \quad \because S=0$. I is thus a

decreasing function so that $\forall\, I > 0$ and $\forall\, I < 0$ along this axis, every solution tends towards the origin along this line. This is seen in figure 3.2 below. In A, $\frac{dS}{dt} > 0, \quad \forall\, I > 0$. Thus, in A $(-\infty < S < 0)$ S is increasing. It follows that in F, S is decreasing.

A similar consideration yields the figure below showing the flow direction of S and I in each section. The computer algebra system generated figure 3.3 was achieved using '*pplane8'* program in conjunction with *Matlab* 7.10.0.499 (R2010a). It will also be used for the phase plane diagram. The program *pplane* 8 was accessed on 13/05/2013 from http://math.rice.edu/~dfield/.

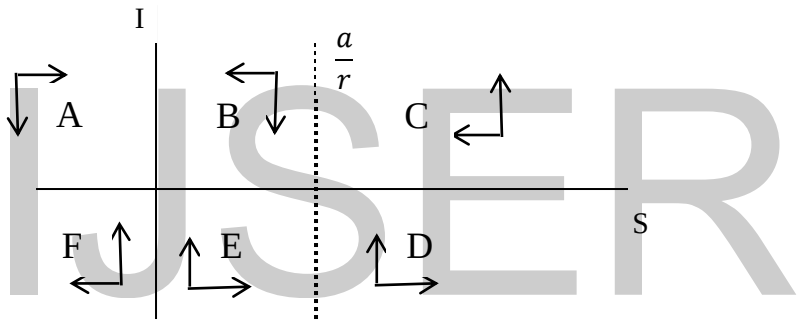

Figure 3.2 The null clines for the system showing the flow direction for the different sections.

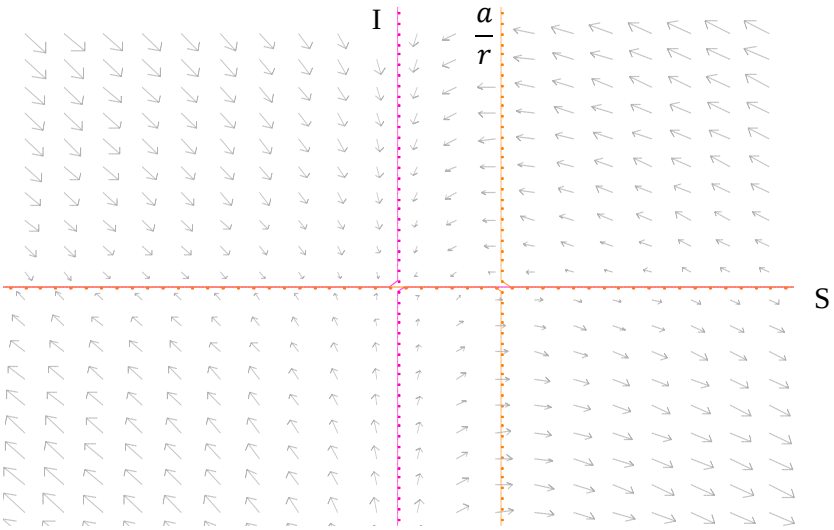

Figure 3.3 A computer generated version of fig 3.2. The coloured lines indicate the null clines while the arrows indicate the flow direction for each sector.

3.2.3 PHASE PORTRAIT

The **phase-portrait** for the autonomous system (1.9) is the geometrical representation of all its trajectories (solution curve) on the phase plane. This **phase plane** is a two-dimensional space with coordinates for the dependent variables x and y. Given that one may not display all the trajectories, but a sketch of it, it is standard practice to use phase portrait to denote a sketch of it (Glenn, 2005).

The differential equation (relating the dependent variables) for the phase portrait for (1.9) is given by

$$\frac{dy}{dx} = \frac{\frac{dy}{dt}}{\frac{dx}{dt}} = \frac{g(x,y)}{f(x,y)} \tag{1.16}$$

As t increases, we cannot tell the direction of evolution of the phase path from(1.16). This drawback is settled by considering the sign of $f(x,y)$ and $g(x,y)$ at any reference point as this gives the direction through that point. Theorem 1 above guarantees that adjacent paths have the same direction.

The system representing the dynamics of the disease spread is

$$\begin{aligned} \frac{dS}{dt} &= -rSI \\ \frac{dI}{dt} &= rSI - aI \end{aligned} \tag{1.17}$$

Equation (1.17) cannot be solved for an explicit formula representing the solution.

Using (1.16), (1.17) yields $\frac{dI}{dS} = \frac{(rS - a)}{-rSI}$ so that the differential equation for the phase portrait is

$$\frac{dI}{dS} = \frac{a}{rS} - 1 \tag{1.18}$$

which upon integration yields

$$I = \frac{a}{r}\log S - S + K \tag{1.19}$$

$$I = \sigma \log S - S + K \tag{1.20}$$

where $\sigma = \frac{a}{r}$ and K is the arbitrary constant of integration.

Equation (1.20) gives the family of curves constituting the phase portrait.

The null cline analysis of the previous section gives a visual representation of the flow of the susceptible and infective compartments. Given that the population of the different compartments of the models does not permit negative values, the domain of interest is the quadrant $S \geq 0$, $I \geq 0$.

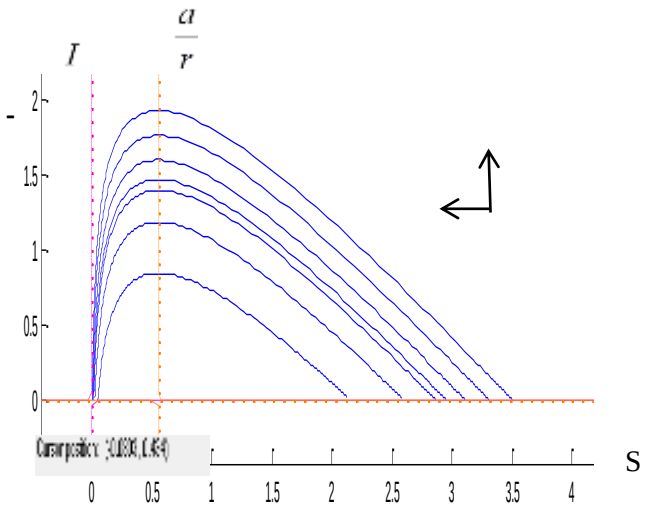

Figure 3.4 Phase portrait for the SIR system

Further result of interest.

Using (1.2) to determine K in(1.20), yields

$$K = I_0 - \sigma \log S_0 + S_0 \tag{1.21}$$

But $I_0 + S_0 = N$ [from (1.2) and(1.3)]

So that (1.20) becomes $I = \sigma \log S - S + N - \sigma \log S_0$ (1.22)

Setting S_∞ as the limiting value of S as $t \to \infty$ and $I \to 0$ as $t \to \infty$, (1.22)becomes

$$N - \sigma \log S_0 = S_\infty - \sigma \log S_\infty \tag{1.23}$$

This upon rearranging and exponentiation yields

$$S_\infty = S_0 e^{-\left(\frac{N - S_\infty}{\sigma}\right)} \tag{1.24}$$

$$\Rightarrow \quad S_\infty > 0, \quad \text{since } S_0 > 0 \text{ and } e^{-\left(\frac{N - S_\infty}{\sigma}\right)} > 0$$

Thus not everyone contracts the disease. This observation is in sync with observable real life scenario of epidemics where some people do not contract the disease yet they are not immune. Equation (1.23) is the final size equation.

3.2.4 ON R_0, σ AND R

In epidemiology, a threshold quantity is a critical value of the quantity that must be reached or exceeded for a disease to remain endemic or for an epidemic to occur. Hethcote (2005) made the case for three distinct but related threshold quantities. These are the basic reproduction number (R_0), contact number (σ) and the replacement number (R). The replacement number is also referred to as the effective reproduction number (Cintron-Arias A., et al, 2009; Brauer, 2006)

The basic reproduction number R_0 is the average number of secondary infections consequent on the introduction of an infective into a population that is entirely susceptible during the period of infectiousness (Murray, 2002; Hethcote, 2005; Bakare et al, 2012). This simply refers to the number of individuals which a single infective infects during the infectious period in a population of susceptible. Given that it determines the size and duration of epidemics, it is an important epidemiological quantity (Grais et al, 2006). The contact number (σ) is the average number of adequate contacts of an infective during the infectious period. An adequate contact is an interaction with a susceptible which results in an infection while the replacement number (R) is the average number of susceptible infected by an infective during the period of infectiousness (Hethcote, 2005). R may be thought of as the parallel quantity to R_0 for populations that are not wholly susceptible (Grais et al, 2006).

From (1.4) and (1.5)

$$\left(\frac{dI}{dt}\right)_{t=0} = \left(rS_0 - a\right)I_0 \tag{1.25}$$

This represents the situation of the infective compartment at the initial stage. There are 3 possible direction of evolution: $I' = 0,\ I' < 0$ and $I' > 0$

$$\text{For} \quad \left(\frac{dI}{dt}\right)_{t=0} = 0\ , \qquad \left(rS_0 - a\right)I_0 = 0 \tag{1.26}$$

$$rS_0 - a = 0, \quad \because I_0 > 0 \tag{1.27}$$

$$S_0 = \frac{a}{r}, \quad \text{or} \quad \frac{r}{a}S_0 = 1 \tag{1.28}$$

It follows that

$$\text{For} \left(\frac{dI}{dt}\right)_{t=0} < 0, \quad S_0 < \frac{a}{r} \ or \ \frac{r}{a}S_0 < 1 \tag{1.29}$$

$$\text{For} \left(\frac{dI}{dt}\right)_{t=0} > 0, \quad S_0 > \frac{a}{r} \ or \ \frac{r}{a}S_0 > 1 \tag{1.30}$$

If it is assumed that everyone in the population is initially susceptible i.e. $S_0 \approx N$ then, $R_0 = \frac{rN}{a}$.

There will be an epidemic if and only if $R_0 > 1$ and a necessary condition for the disease to fizzle out of the population is $R_0 < 1$. $R_0 = \frac{rN}{a}$ is the basic reproduction number while $R = \frac{rS_0}{a}$ is the replacement number. Observe that in a population that is not wholly susceptible, the replacement number becomes the threshold parameter of choice. Consequently, there will be an epidemic if $R > 1$ (i.e. every infective infects more than one person on average), no epidemic if $R < 1$ (i.e. the disease will die out) while the disease will remain endemic if $R = 1$

3.2.5 COMMENT ON QUALITATIVE ANALYSIS

Without explicitly solving the system of differential equations(1.17), integrating the null cline analysis with the phase portrait gives an inkling of the long term behaviour of the trajectories (solution curves).

What results can be elicited from the phase plane portrait of figure 3.4? The line $S = \frac{a}{r}$ divides the phase plot into two parts so that if S_0 is to its left, $R_0 < 1$ and S_0 to its right implies $R_0 > 1$. Thus, for any initial condition (1.2) with $S_0 > \frac{a}{r}$ *or* $\frac{r}{a} S_0 > 1$, the susceptible decreases as time progresses but does not get to zero [see (1.24)] while the infective initially increases from I_0, gets to a maximum at $S = \frac{a}{r}$ and then decreases to zero. Observe that as the infective is increasing, the susceptible is decreasing and when $S = \frac{a}{r}$ the infective compartment is neither increasing nor decreasing. Given that $I(t) > I_0$ for any $t > 0$ an epidemic occurs. If however, $S_0 < \frac{a}{r}$ the possibility of an epidemic is ruled out as the infective population decreases from the onset.

3.3 STABILITY ANALYSIS

$$J(S,I)=\begin{pmatrix} -rI & -rS \\ rI & rS-a \end{pmatrix} \tag{1.31}$$

$$J(S^*,I^*)=\begin{pmatrix} -rI & -rS \\ rI & rS-a \end{pmatrix}_{(S^*,0)} \tag{1.32}$$

$$=\begin{pmatrix} 0 & -rS^* \\ 0 & rS^*-a \end{pmatrix}$$

If A be the Jacobian matrix, then, for the characteristic equation for the eigenvalues $(\gamma_i,\ i=1,2)$ of A, we have $P(\gamma)=\gamma^2-(trace\ A)\gamma+\det A=0$

So that $$\gamma^2-(rS^*-a)\gamma=0 \tag{1.33}$$

$$\Rightarrow \quad \gamma_1=0,\ \gamma_2=rS^*-a$$

$$\gamma_2<0 \text{ if } S^*<\tfrac{a}{r} \text{ and } \gamma_2>0 \text{ if } S^*>\tfrac{a}{r} \tag{1.34}$$

It follows that the system will be stable whenever $S^*<\frac{a}{r}$ and unstable otherwise in the invariant region $S>0, I>0$

From figure 3.4 it is important to notice that solutions that begin from any point $S_0<\frac{a}{r}$ does not get blown away as time evolves but rather stays close to the equilibrium point S^* while on the other hand solutions beginning from any point $S_0>\frac{a}{r}$ gets blown further away from the equilibrium point as time progresses

3.4 REGIONAL MEASLES REPORTED CASES

The figure below gives a visual representation of the incidence of measles in the regions under consideration for the period under study.

Nigeria is a country with 36 states and a federal capital territory divided into 6 geo-political zones. For the purpose of this study, the state with the highest measles incidence in each zone was chosen as its representative. See appendix B for the breakdown of the spread of the incidence of the disease.

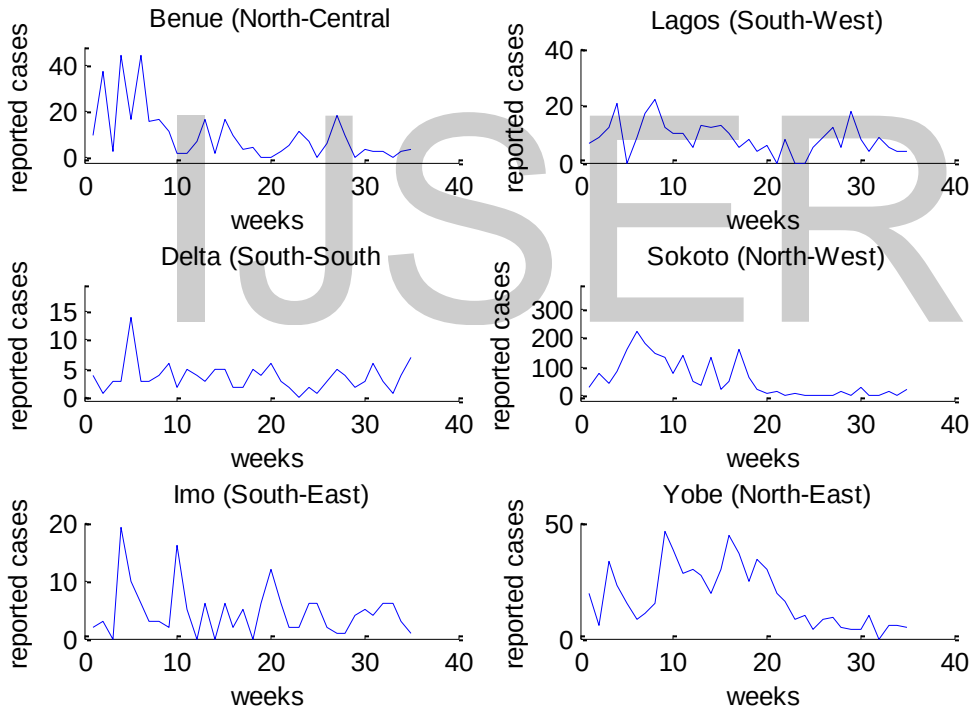

Figure 3.5 The reported cases of measles in the regions

4.0 CHAPTER FOUR

This concluding chapter presents the numerical simulation results for the three models considered in this study and discusses their import. It also gives an indication of possible areas of further exploration.

4.1 NUMERICAL SIMULATION

Otto and Denier (2005) observed that there are many problems which simply do not have analytical solutions or those whose exact solution is beyond our current state of knowledge. The models under consideration fall within the former category. In cases as this, it is prudent to resort to numerical integration schemes (Keeling and Rohani, 2008).

To enhance appropriate comparison between the models and the measles epidemiological data, the models were simulated using the inbuilt numerical integrator ode45 of *Matlab*. This solver employs the Runge-Kutta 4 Dormand Prince algorithm. An invaluable insight into the mechanisms of the different *Matlab* ode solvers is available from Shampine and Reichelt (1997).

For the numerical simulations, the table below gives the estimates of parameters used from literature.

Parameter	Estimate	Source
R_0	18	Earn, 2004
a	$\frac{1}{5}$ days^{-1}	Lloyd & May, 1995
λ	$\frac{1}{8}$ days^{-1}	Lloyd & May, 1995
$L = \frac{1}{\mu}$	53	WHO [42]

Table 1 Epidemiology parameter values for measles from literature

4.2 SIMULATIONS FOR SIR MODEL

The model (1.1) was used for the simulations of this section. The initial conditions together with the parameter values used are given below for each region. The first two figures for each region are the plots of the disease dynamics assuming a wholly susceptible population with the introduction of one infective. The choice of truncating the time of evolution for the plots of the dynamics for the different compartments was informed by the manifested steady form of the dynamics from about the 5th week.

The 3rd and 4th figures on the other hand captured the case of the population not being wholly susceptible. The extended time frame beyond the limits of the epidemiology data for these plots was to allow the computer simulation of the complete evolution of the disease dynamics

The measles trend in Nigeria (figure 1.1) made the case for the prior long occurrence of the disease in the country so that the population of the regions cannot be wholly susceptible given that measles confers lifelong immunity. Following Earn (2004) I_0 was estimated as the number of cases in the first week times the infectious period as a proportion of the length of the week while $S_0 = 0.065N$.

R_0	I_0	S_0	r	a
18	1	$N-1$	$\frac{aR_0}{N}$	$\frac{1}{5}\ \text{days}^{-1} = \frac{7}{5}\text{weeks}^{-1}$

Table 2 Initial and parameter values used with the SIR model for a wholly susceptible population. Other values are given with the graphs below

R_0	S_0	r	a
18	$0.065N$	$\frac{aR_0}{N}$	$\frac{1}{5}\ \text{days}^{-1} = \frac{7}{5}\text{weeks}^{-1}$

Table 3 Initial and parameter values used with the SIR model for a population not wholly susceptible. Other values are given with the graphs below

4.2.1 BENUE

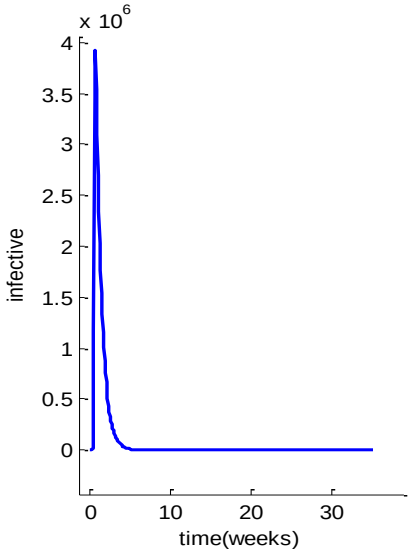

Figure 4.1 The SIR epidemic curve for Benue with N=5037998 and the values of table 2

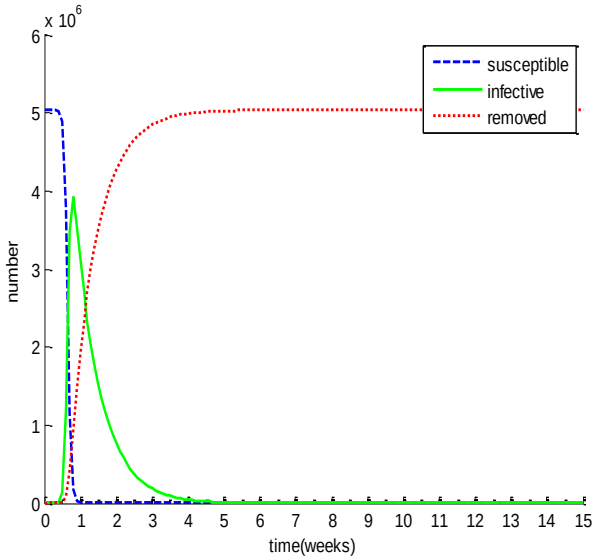

Figure 4.2 The SIR dynamics of the compartments for Benue with N=5037998 and the values of table 2

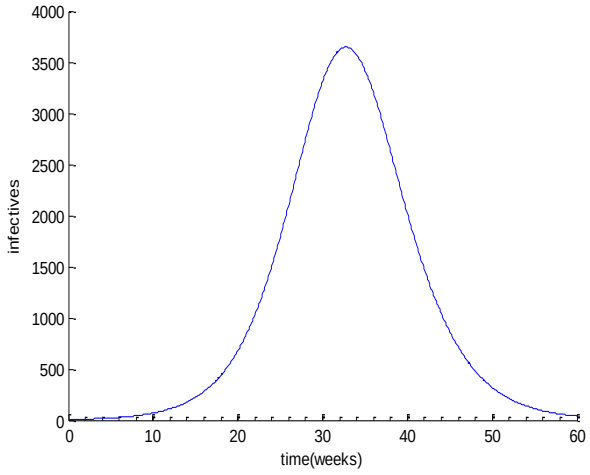

Figure 4.3 The SIR epidemic curve for Benue with N=5037998, $I_0 = 9\left(\frac{5}{7}\right)$ and the values of table 3

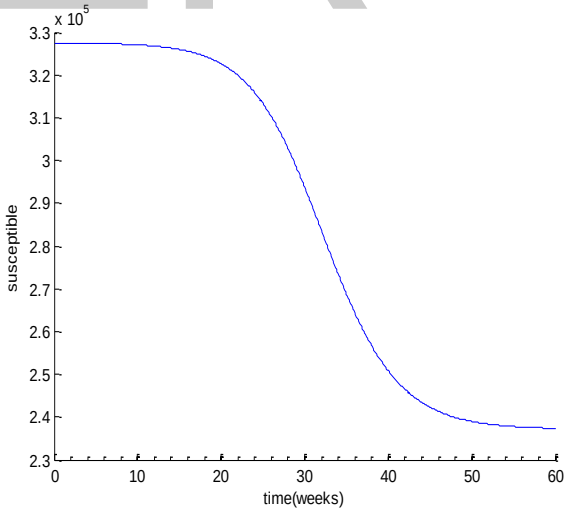

Figure 4.4 The SIR susceptible curve for Benue with N=5037998, $I_0 = 9\left(\frac{5}{7}\right)$ and the values of table 3

4.2.2 DELTA

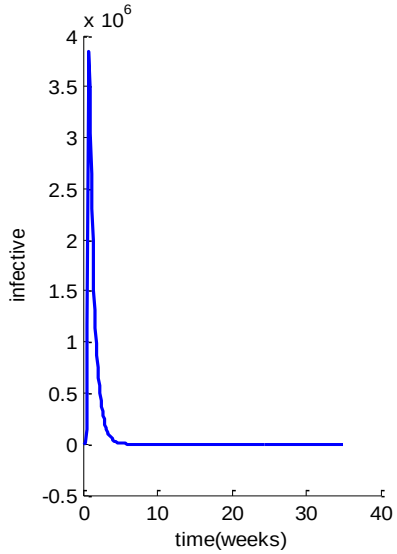

Figure 4.6 The SIR epidemic curve for Delta with N=4950985 and the values of table 2

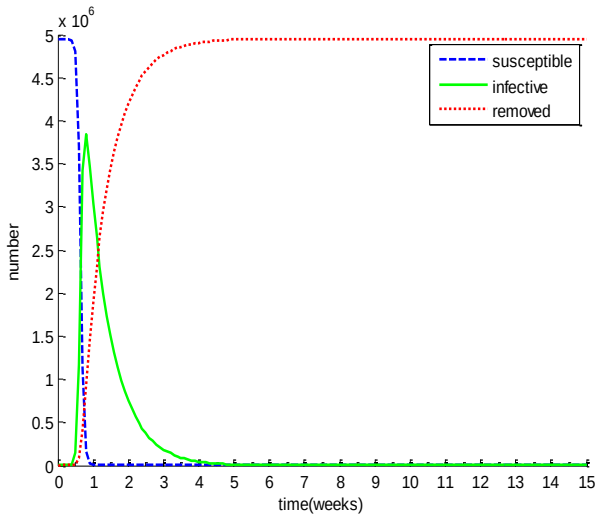

Figure 4.5 The SIR dynamics of the compartments for Delta with N=4950985 and the values of table 2

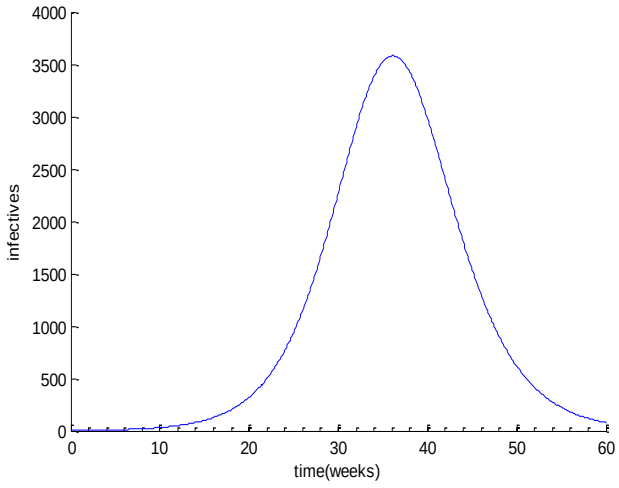

Figure 4.8 The SIR epidemic curve for Delta with N=4950985, $I_0 = 4\left(\frac{5}{7}\right)$ and the values of table 3

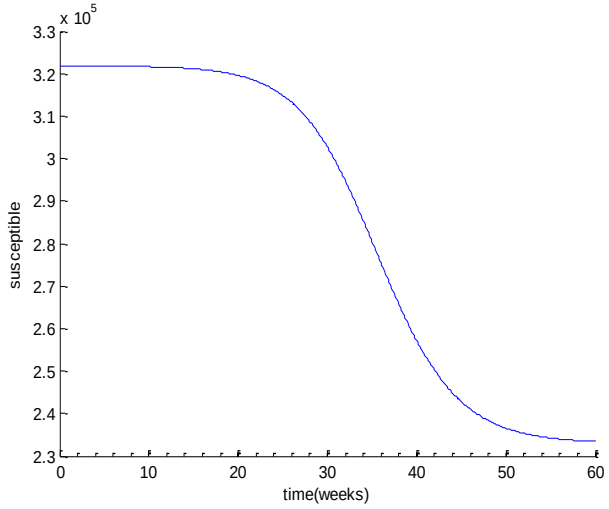

Figure 4.7 The SIR susceptible curve for Delta with N=4950985, $I_0 = 4\left(\frac{5}{7}\right)$ and the values of table 3

4.2.3 IMO

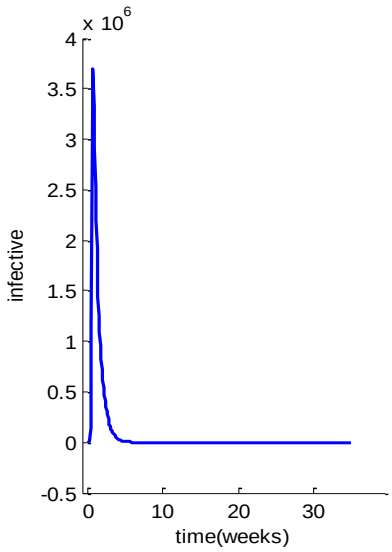

Figure 4.10 The SIR epidemic curve for Imo with N=4753481 and the values of table 2

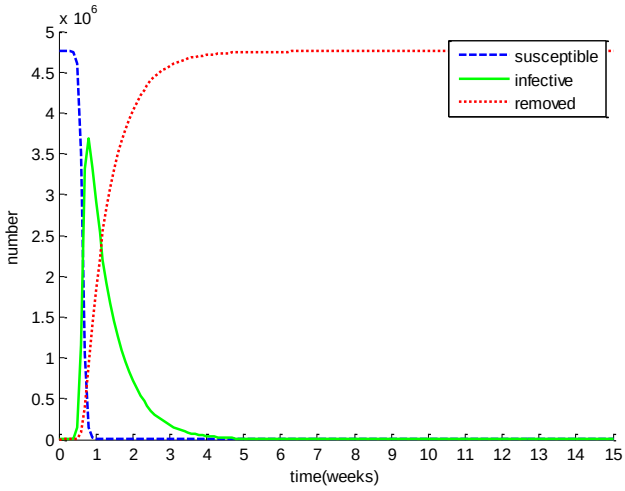

Figure 4.9 The SIR dynamics of the compartments for Imo with N=4753481 and the values of table 2

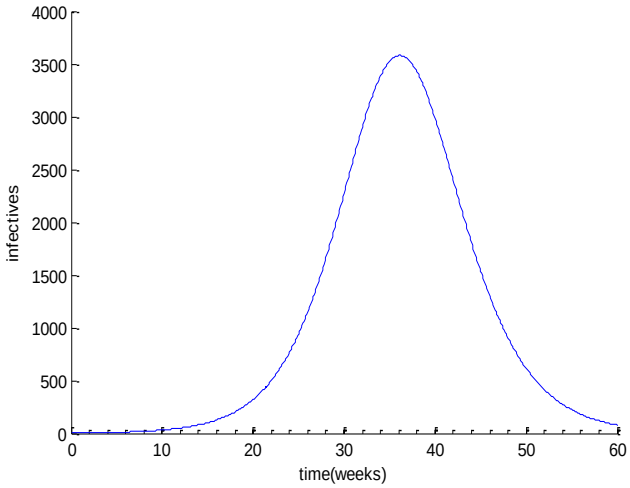

Figure 4.12 The SIR epidemic curve for Imo with N=4753481, $I_0 = 2\left(\frac{5}{7}\right)$ and the values of table 3

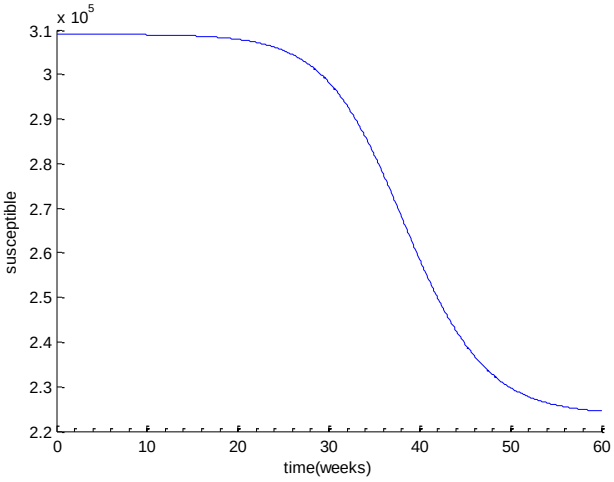

Figure 4.11 The SIR susceptible curve for Imo with N=4753481, $I_0 = 2\left(\frac{5}{7}\right)$ and the values of table 3

4.2.4 LAGOS

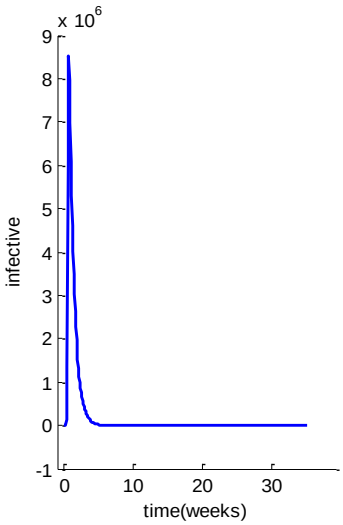

Figure 4.14 The SIR epidemic curve for Lagos with N=10888631 and the values of table 2

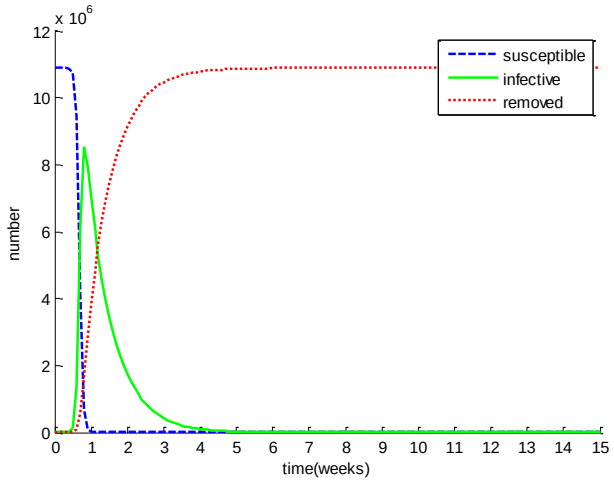

Figure 4.13 The SIR dynamics of the compartments for Lagos with N=10888631 and the values of table 2

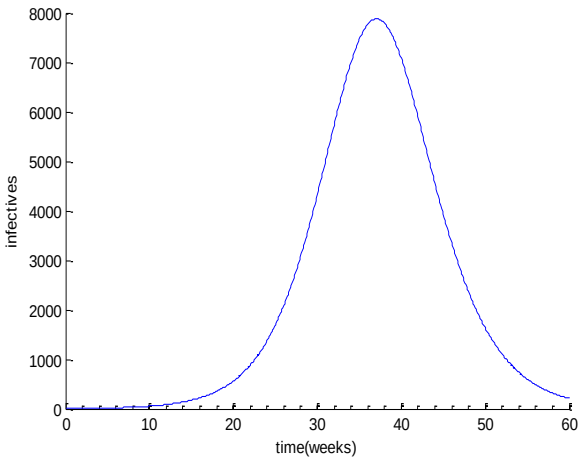

Figure 4.16 The epidemic curve for SIR model for Lagos with N=10888631, $I_0 = 7\left(\frac{5}{7}\right)$ and the values of table 3

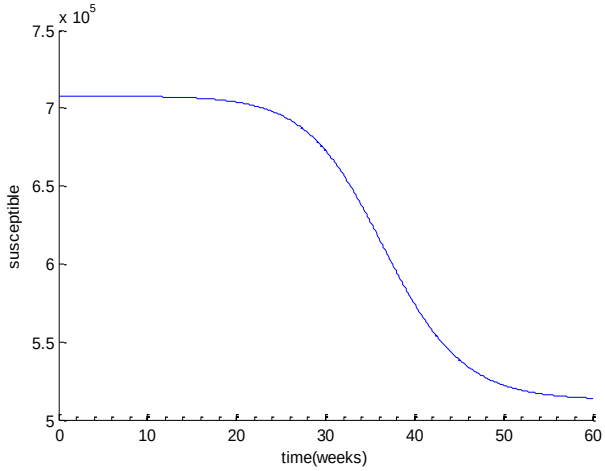

Figure 4.15 The SIR susceptible curve for Lagos with N=10888631, $I_0 = 7\left(\frac{5}{7}\right)$ and the values of table 3

4.2.5 SOKOTO

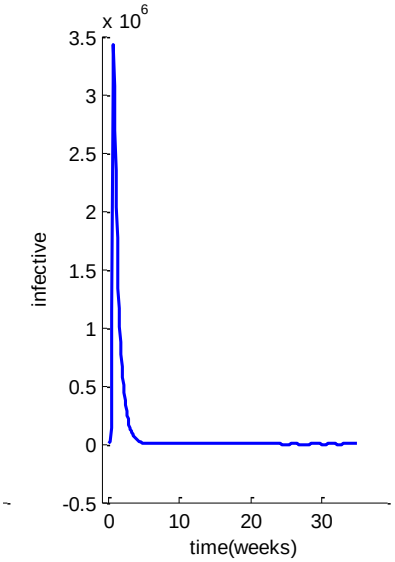

Figure 4.18 The SIR epidemic curve for Sokoto with N=4414410 and the values of table 2

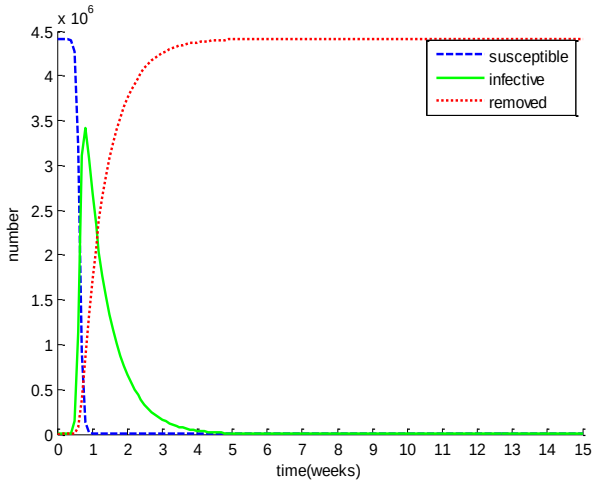

Figure 4.17 The SIR dynamics of the compartments for Sokoto with N=4414410 and the values of table 2

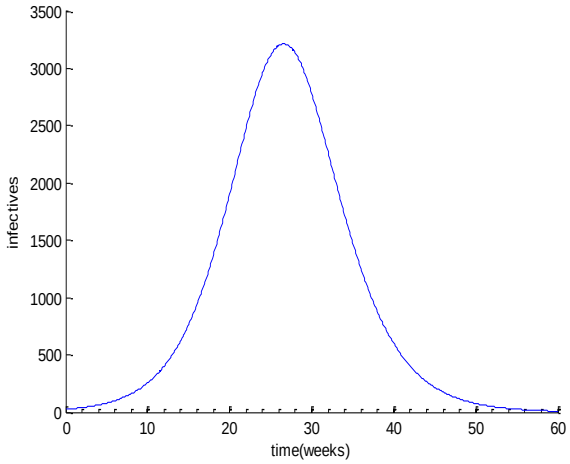

Figure 4.20 The SIR epidemic curve for Sokoto with N=4414410, $I_0 = 34\left(\frac{5}{7}\right)$ and the values of table 3

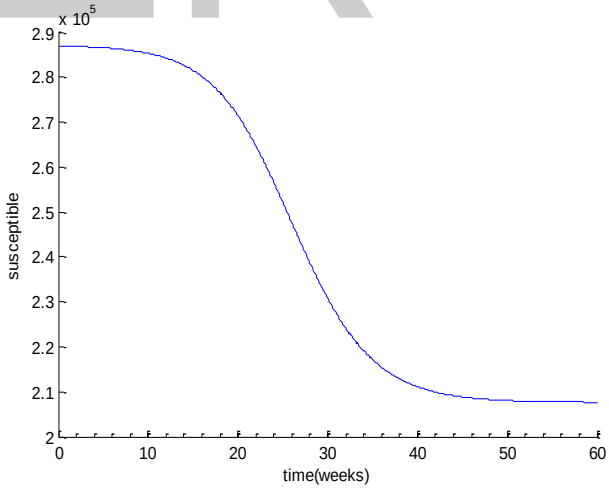

Figure 4.19 The SIR susceptible curve for Sokoto with N=441441 $I_0 = 34\left(\frac{5}{7}\right)$ and the values of table 3

4.2.6 YOBE

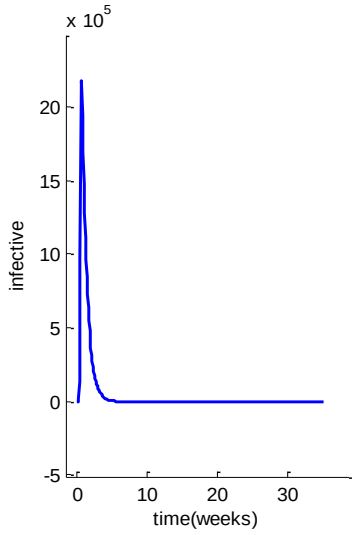

Figure 4.21 The SIR epidemic curve for Yobe with N=2853828 and the values of table 2

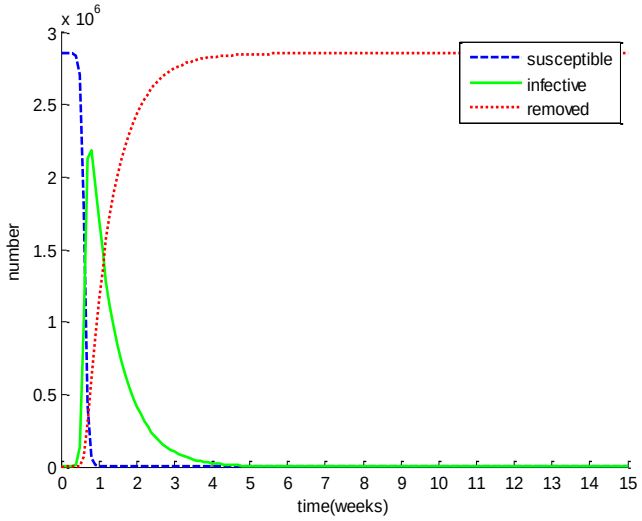

Figure 4.22 The SIR dynamics of the compartments for Yobe with N=2853828 and the values of table 2

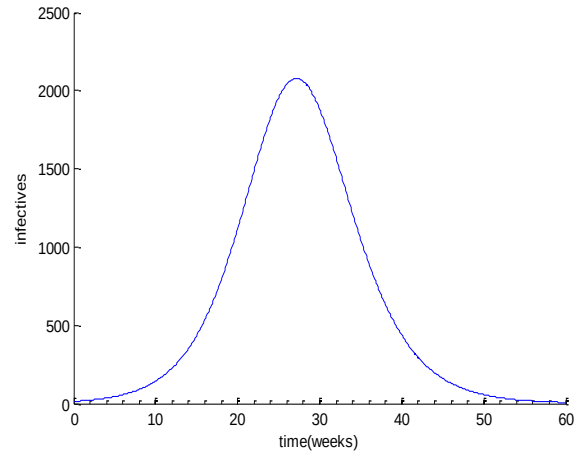

Figure 4.23 The SIR epidemic curve for Yobe with N=2853828, $I_0 = 19\left(\frac{5}{7}\right)$ and the values of table 3

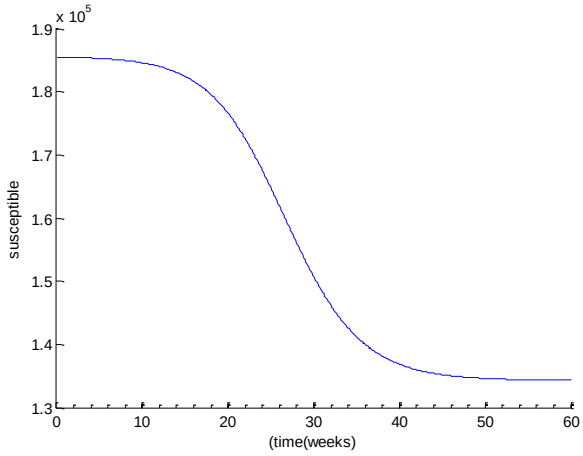

Figure 4.24 The SIR susceptible curve for Yobe with N=2853828, $I_0 = 19\left(\frac{5}{7}\right)$ and the values of table 3

4.3 COMMENT ON SIMULATIONS FOR SIR MODEL

The first two graphs of this section for each region show a steep exponential growth curve for the infective population consequent on the assumption of a wholly susceptible population with only an infective. This is removed from the reality of the persistent presence of the disease in the population prior to 2012 so that not the whole population is susceptible. It is however insightful in showing that should the population be wholly susceptible, the intensity of the disease is expected to be severe given the steepness of the curve though the disease will not be in the population for a long time. This underscores the observation of Murray (2002) that though the SIR is a basic model, some highly relevant comments about epidemics can be made.

This model together with the assumption of a not wholly susceptible population is an improvement of the previous. There is an observed delay before the evolution of the epidemic curves as can be seen in figures (4.3, 4.8, 4.11, 4.15, 4.20, 4.24) and the steepness observed in the previous simulations gave way to a gradual but steady exponential growth of the epidemic curve. Compared to the incidence of the disease in the regions, it fairs poorly in adequately describing the scenario. It is to be noted though that the epidemic curves are in agreement with the result of the qualitative analysis of chapter 2 i.e. the infective increases to a maximum and then declines to zero.

It is pertinent to observe that the SIR and SEIR models without vital dynamics lacked the capacity to capture the observed seemingly cyclic repetition observed in infectious diseases. This is attributable to the susceptible compartment being continually depleted without a source of replenishment of its members. The consequence of this is that “things therefore go as though only one epidemic were to be observed from only one wave of susceptible that ultimately goes to extinction” (Trottier and Philippe, 2002).

4.4 SIMULATIONS FOR SEIR (WITHOUT VITAL DYNAMICS) MODEL

The model (1.6) was used for the simulations of this section. The initial conditions together with the parameter values used are given below for the regions. The first two figures for the regions are the plots of the disease dynamics assuming a wholly susceptible population with the introduction of one infective. The choice of truncating the time of evolution for these plots was informed by the manifested steady form of the dynamics from about the 12th week.

The 3rd and 4th plots are the dynamics for the case of the population not being wholly susceptible. The extended time frame beyond the limit of the epidemiology data was to allow the complete simulation of the evolution of the disease dynamics.

The estimation of the infective and susceptible at time $t=0$ follows Earn (2004) i.e. I_0 was estimated as the number of cases in the first week times the infectious period as a proportion of the length of the week while $S_0 = 0.065N$. Lloyd and May (2006) gave an estimate of the exposed at time $t=0$ as $\frac{aI_0}{\lambda}$. See the paper for the justification of this estimate.

R_0	I_0	E_0	S_0	r	λ	a
18	1	$\frac{aI_0}{\lambda}$	$N-1$	$\frac{aR_0}{N}$	$\frac{1}{8}days^{-1} = \frac{7}{8}week^{-1}$	$\frac{1}{5}\ \text{days}^{-1} = \frac{7}{5}\text{weeks}^{-1}$

Table 4 The initial and parameter values used with the SEIR model for a wholly susceptible population. Other values are given with the graphs below

R_0	S_0	E_0	r	λ	a
18	$0.065N$	$\frac{aI_0}{\lambda}$	$\frac{aR_0}{N}$	$\frac{1}{8}days^{-1} = \frac{7}{8}week^{-1}$	$\frac{1}{5}\ \text{days}^{-1} = \frac{7}{5}\text{weeks}^{-1}$

Table 5 The initial and parameter values used with the SEIR model for a population not wholly susceptible. Other values are given together with the graphs below

4.4.1 BENUE

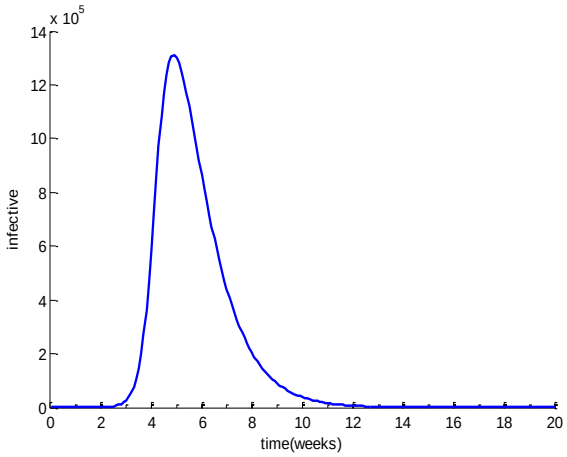

Figure 4.26 The SEIR epidemic curve for Benue with N=5037998 and the values of table 4

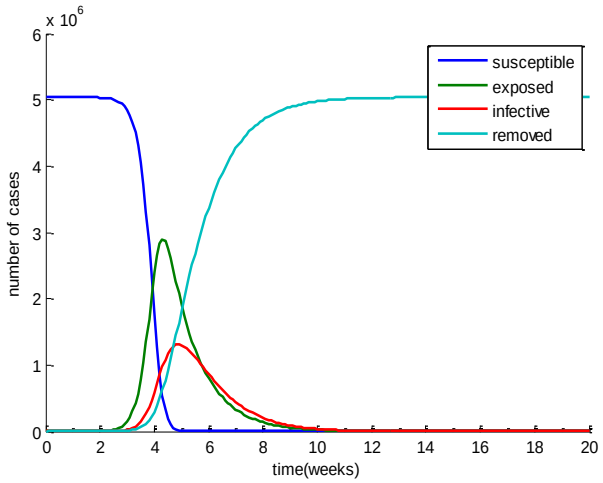

Figure 4.25 The SEIR dynamics of the compartments for Benue with N=5037998 and the values of table 4

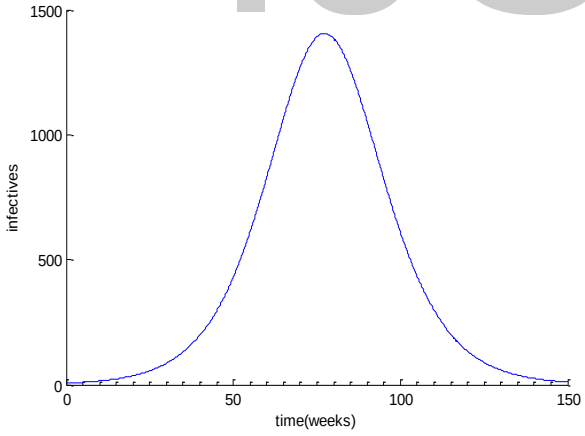

Figure 4.27 The SEIR epidemic curve for Benue with N=5037998, $I_0 = 9\left(\frac{5}{7}\right)$ and the values of table 5

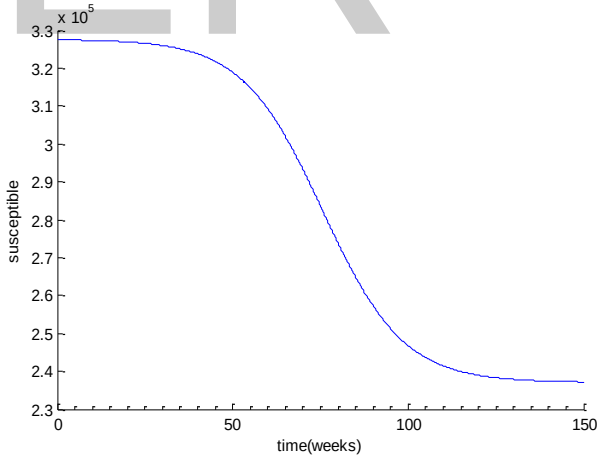

Figure 4.28 The SEIR susceptible curve for Benue with N=5037998, $I_0 = 9\left(\frac{5}{7}\right)$ and the values of table 5

4.4.2 DELTA

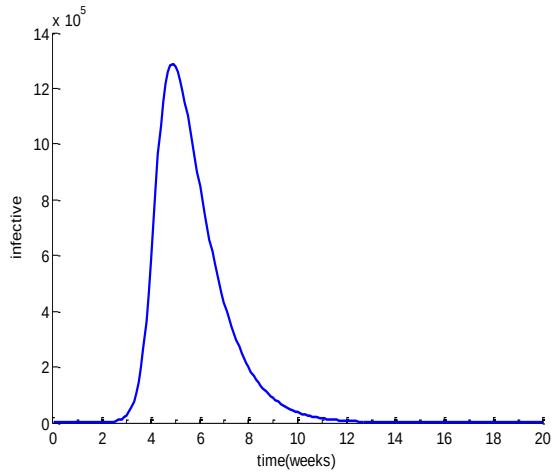

Figure 4.29 The SEIR epidemic curve for Delta with N=4950985 and the values of table 4

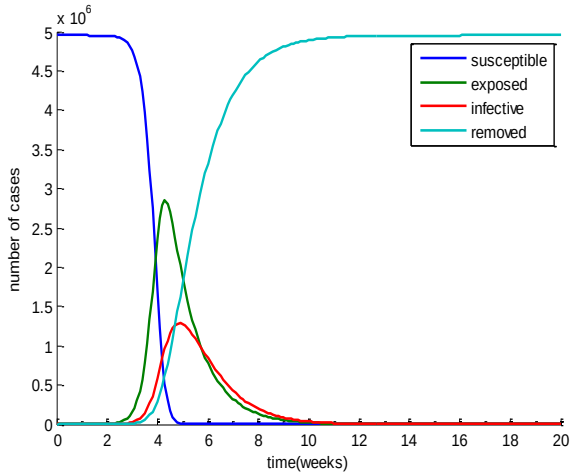

Figure 4.30 The SEIR dynamics of the compartments for Delta with N=4950985 and the values of table 4

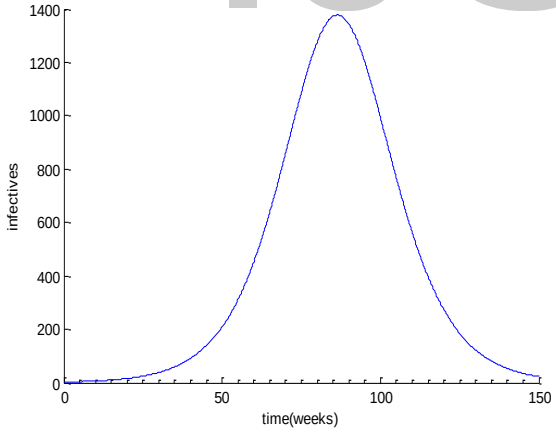

Figure 4.32 The SEIR epidemic curve for Delta with N=4950985, $I_0 = 4\left(\frac{5}{7}\right)$ and the values of table 5

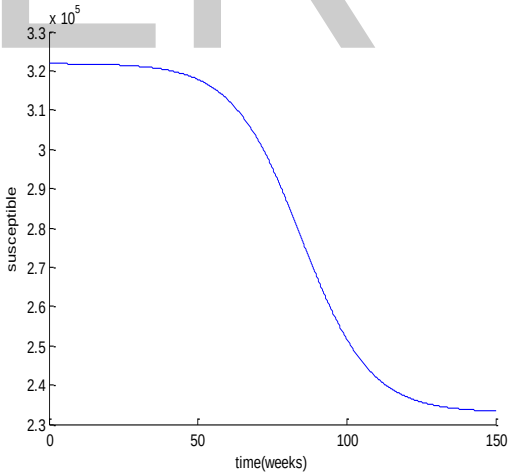

Figure 4.31 The SEIR susceptible curve for Delta with N=4950985, $I_0 = 4\left(\frac{5}{7}\right)$ and the values of table 5

4.4.3 IMO

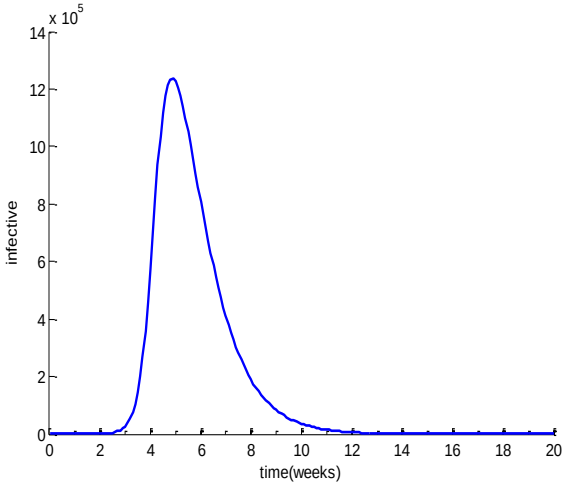

Figure 4.34 The SEIR epidemic curve for Imo with N=4753481 and the values of table 4

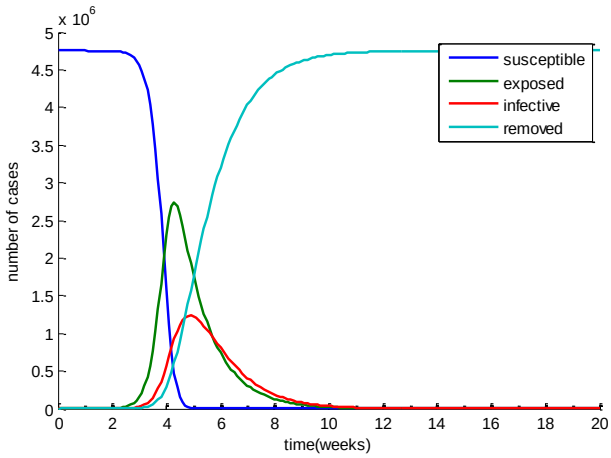

Figure 4.33 The SEIR dynamics of the compartments for Imo with N=4753481 and the values of table 4

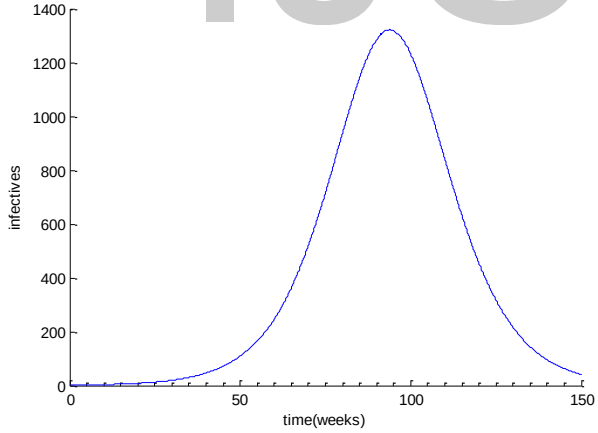

Figure 4.36 The SEIR epidemic curve for Imo with N=4753481, $I_0 = 2\left(\frac{5}{7}\right)$ and the values of table 5

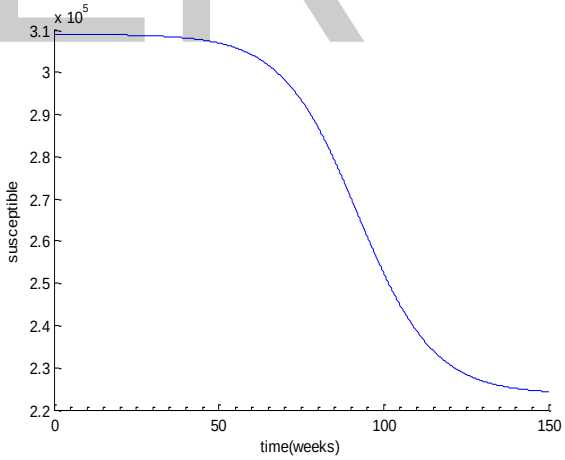

Figure 4.35 The SEIR susceptible curve for Imo with N=4753481, $I_0 = 2\left(\frac{5}{7}\right)$ and the values of table 5

4.4.4 LAGOS

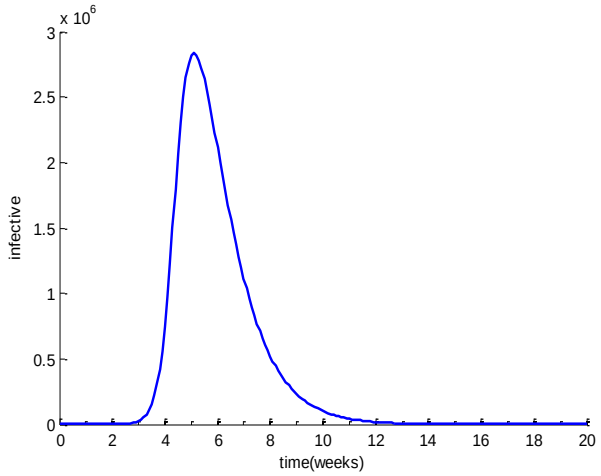

Figure 4.38 The SEIR epidemic curve for Lagos with N=10888631 and the values of table 4

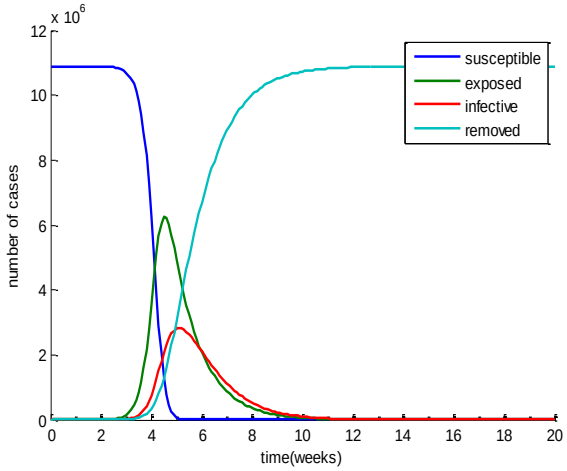

Figure 4.37 The SEIR dynamics of the compartments for Lagos with N=10888631 and the values of table 4

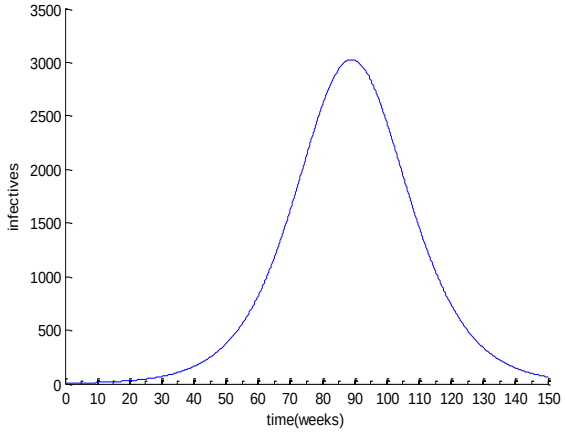

Figure 4.40 The SEIR epidemic curve for Lagos with N=10888631, $I_0 = 7\left(\frac{5}{7}\right)$ and the values of table 5

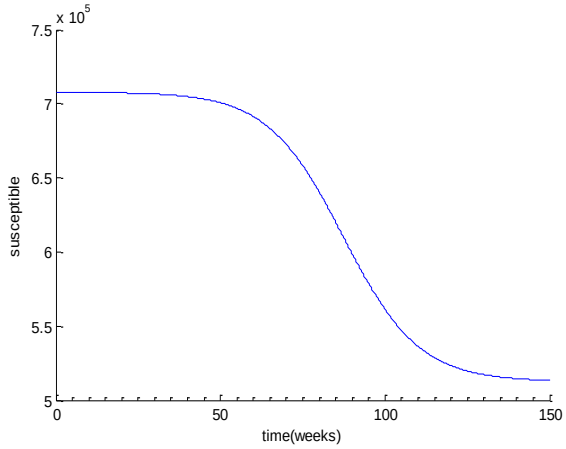

Figure 4.39 The SEIR susceptible curve for Lagos with N=10888631, $I_0 = 7\left(\frac{5}{7}\right)$ and the values of table 5

4.4.5 SOKOTO

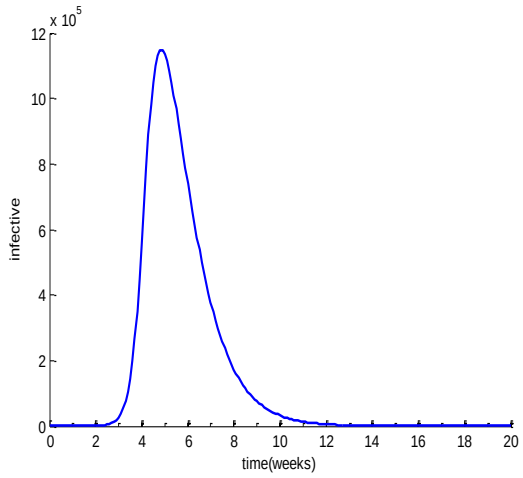

Figure 4.41 The SEIR epidemic curve for Sokoto with N=4414410 and the values of table 4

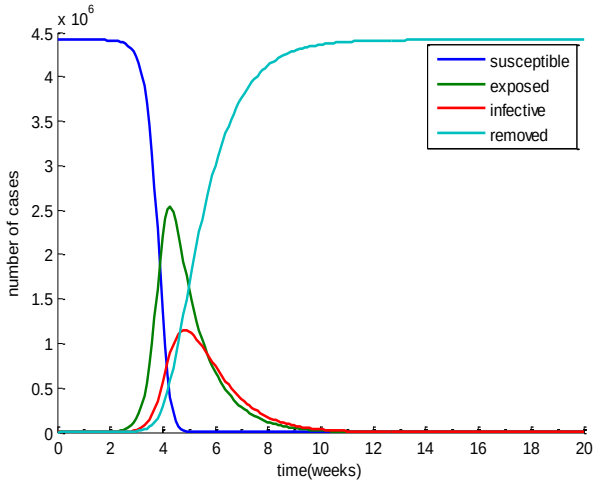

Figure 4.42 The SEIR dynamics of the compartments for Sokoto with N=4414410 and the values of table 4

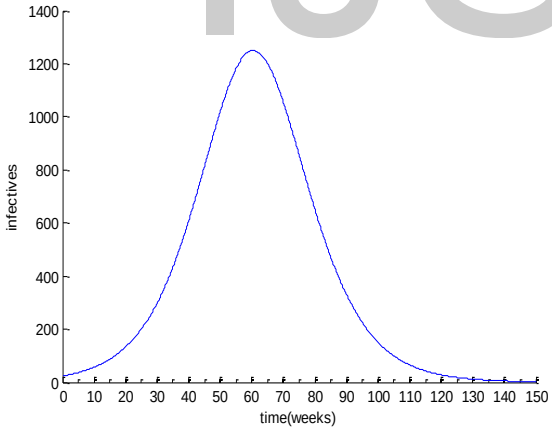

Figure 4.44 The SEIR epidemic curve for Sokoto with N=4414410, $I_0 = 34\left(\frac{5}{7}\right)$ and the values of table 5

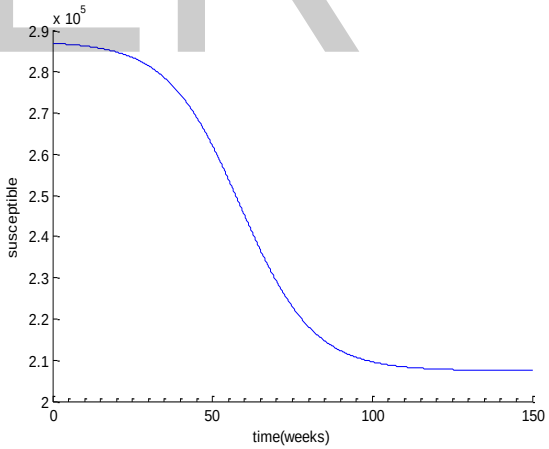

Figure 4.43 The SEIR susceptible curve for Sokoto with N=4414410, $I_0 = 34\left(\frac{5}{7}\right)$ and the values of table 5

4.4.6 YOBE

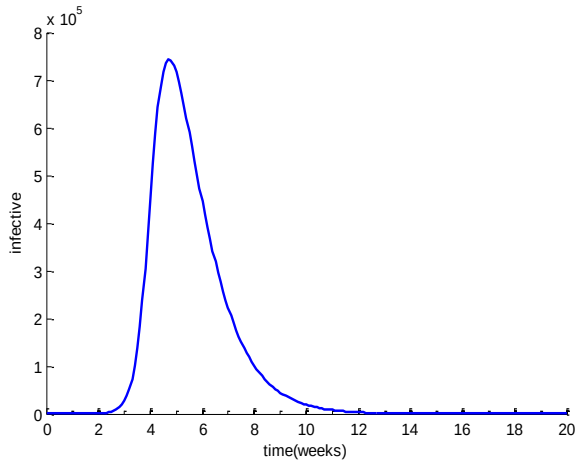

Figure 4.45 The SEIR epidemic curve for Yobe with N=2853828 and the values of table 4

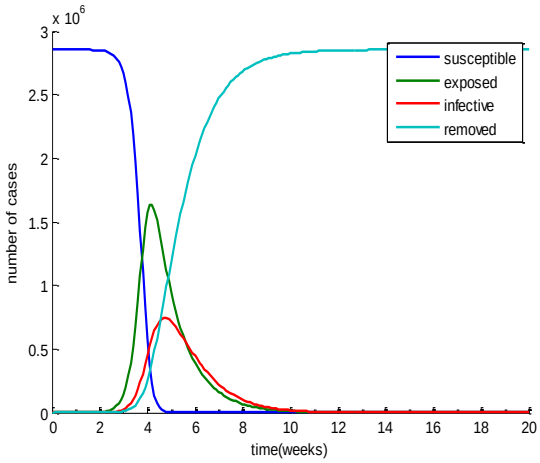

Figure 4.46 The SEIR dynamics of the compartments for Yobe with N=2853828 and the values of table 4

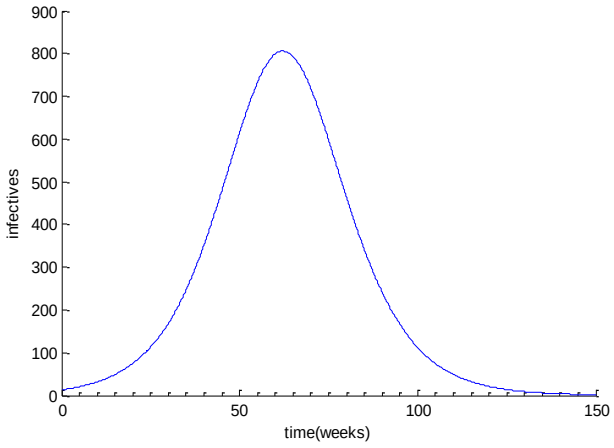

Figure 4.47 The SEIR epidemic curve for Yobe with N=2853828, $I_0 = 19\left(\frac{5}{7}\right)$ and the values of table 5

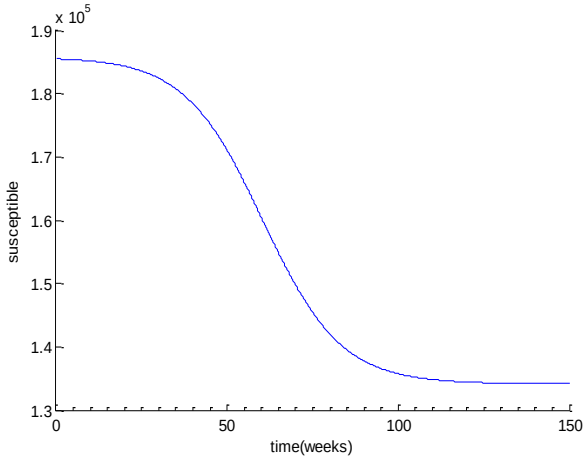

Figure 4.48 The SEIR susceptible curve for Yobe with N=2853828, $I_0 = 19\left(\frac{5}{7}\right)$ and the values of table 5

4.5 COMMENT ON SEIR (WITHOUT VITAL DYNAMICS) SIMULATIONS

The assumption of a wholly susceptible population and model (1.6) with the parameters of table 4 generated the first two graphs for the regions in section 4.4. Figures (4.25, 4.30, 4.34, 4.37, 4.41, and 4.45) show the exposed and infective increasing steadily at the same rate as the susceptible gets depleted which in turn impinges on the emergence of the removed. Recall that this model posits that a person who contracts the disease is first exposed before becoming infective. This explains the observed initial simultaneous rise of the exposed and infective. A very small exposed period leads to dynamics close to the prediction of the SIR model. As the exposed period increases, the spread of infection is slowed down and may completely be halted if too many individuals die before joining the infective compartment.

The assumption of a not wholly susceptible population generated the second set of graphs i.e. figures (4.27, 4.28, 4.31, 4.32, 4.35, 4.36, 4.39, 4.40, 4.43, 4.44, 4.47 and 4.48). The first of this set is put together in figure 4.49 below. Observe that each region demonstrates a similar pattern albeit with different rates of evolution and maxima.

Like the SIR model, this model's performance in adequately describing the incidence of measles in the regions is not close to the mark although it still agrees with an initial increase of the infective to a maximum and then its depletion as time evolves.

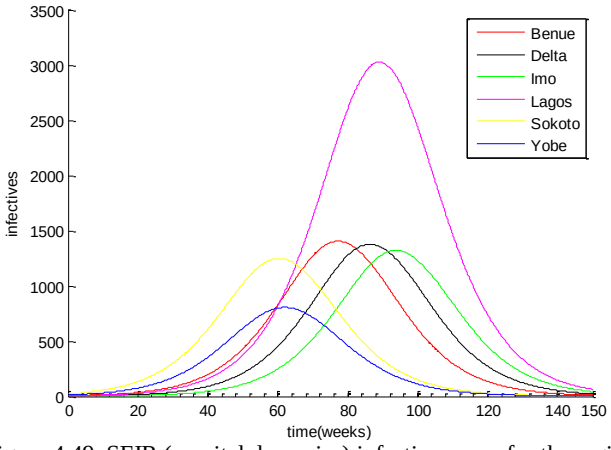

Figure 4.49 SEIR (no vital dynamics) infective curve for the regions

4.6 SIMULATIONS FOR SEIR (WITH VITAL DYNAMICS) MODEL

The model (1.7) was used for these simulations. The initial conditions together with the parameter values used are given below for the regions. The replenishment of the susceptible as provided for by this model guarantees the possibility of a new phase of an infection as is readily observed for infectious diseases. Different time scales were used for the simulations.

R_0	S_0	E_0	r	μ	λ	a
18	$0.065N$	$\frac{aI_0}{\lambda}$	$\frac{aR_0}{N}$	$\frac{1}{53}$	$\frac{1}{8}\,days^{-1} = \frac{7}{8}\,weeks^{-1} = \frac{365}{8}\,years^{-1}$	$\frac{1}{5}\ \text{days}^{-1} = \frac{7}{5}\,\text{weeks}^{-1} = \frac{365}{5}\,years^{-1}$

Table 6 Initial and parameter values used with the SEIR model for a population not wholly susceptible. Other values are given together with the graphs below

4.6.1 BENUE

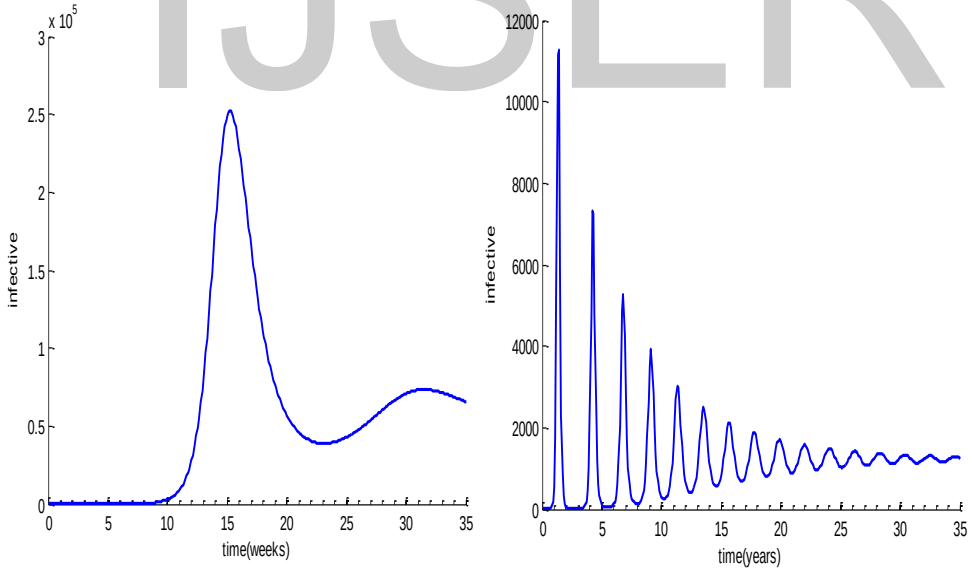

Figure 4.50 The epidemic curve for Benue with N=5037998, $I_0 = 9\left(\frac{5}{7}\right)$ and the values of table 6

4.6.2 DELTA

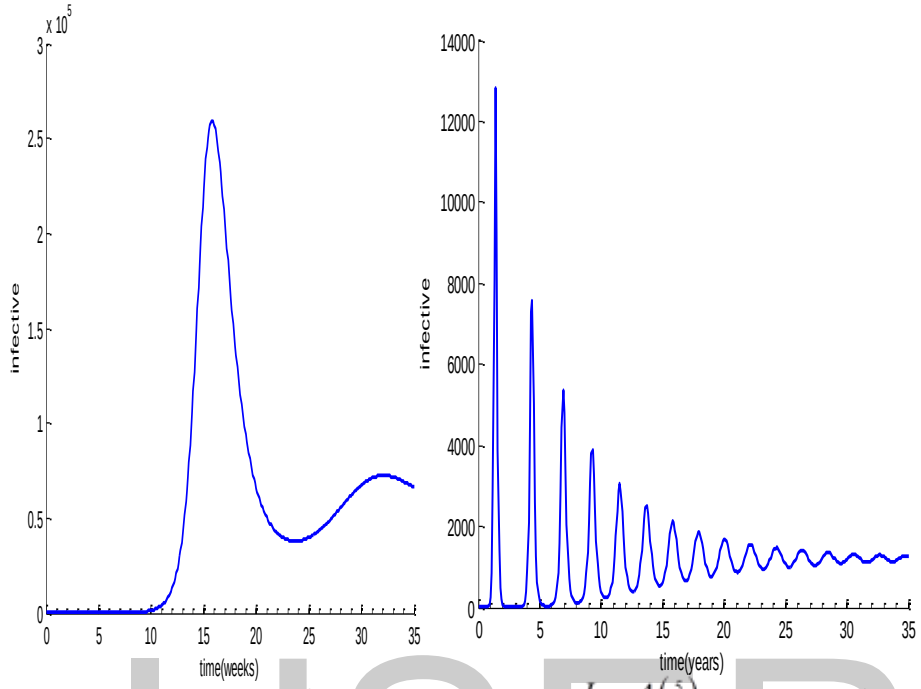

Figure 4.51 The epidemic curve for Delta with N=4950985, $I_0 = 4\left(\frac{5}{7}\right)$ and the values of table 6

4.6.3 IMO

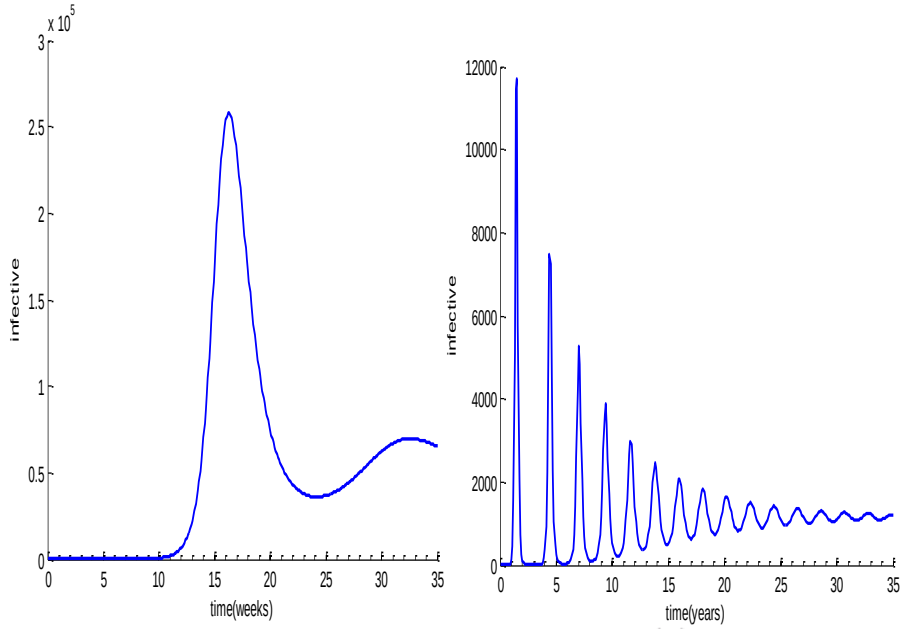

Figure 4.52 The epidemic curve for Imo with N=4753481, $I_0 = 2\left(\frac{5}{7}\right)$ and the values of table 6

4.6.4 LAGOS

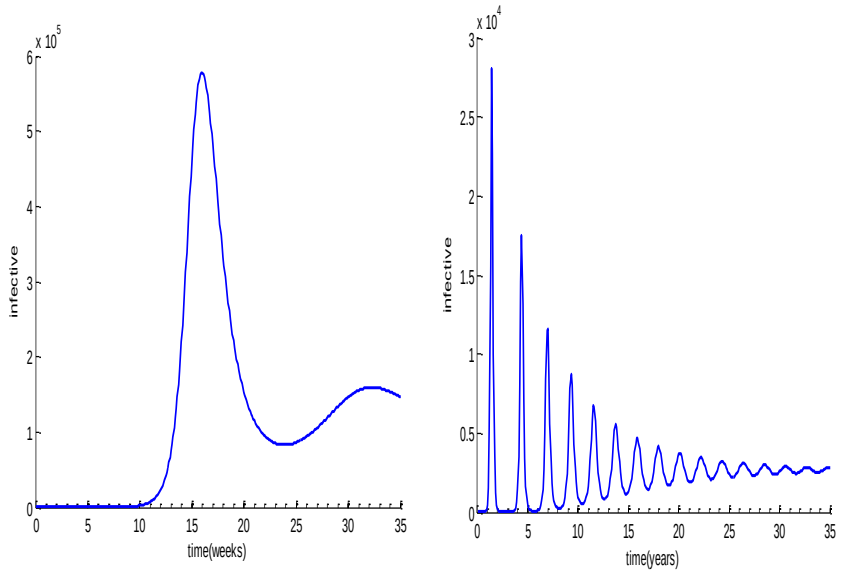

Figure 4.53 The epidemic curve for Lagos with N=10888631, $I_0 = 7\left(\frac{5}{7}\right)$ and the values of table 6

4.6.5 SOKOTO

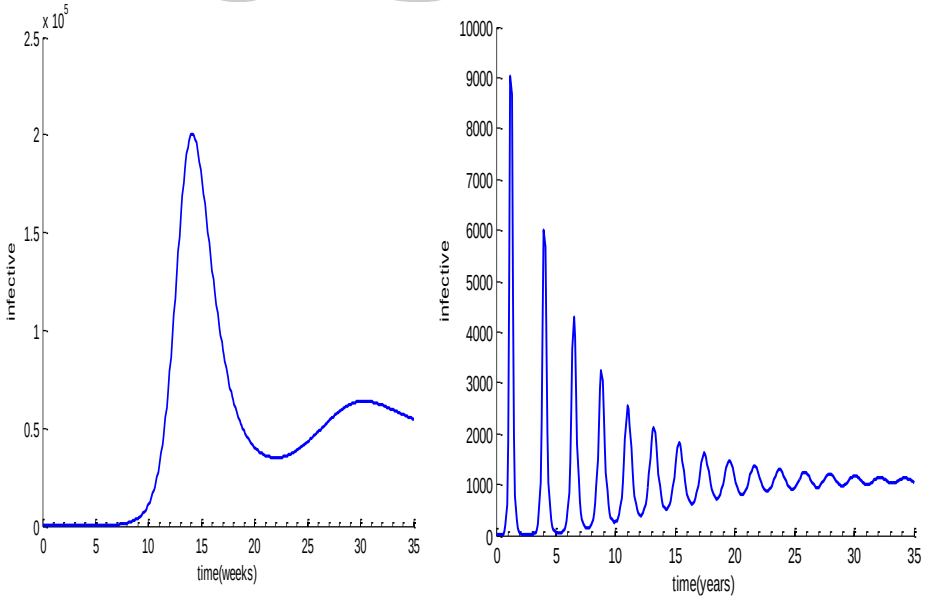

Figure 4.54 The epidemic curve for Sokoto with N=4414410, $I_0 = 34\left(\frac{5}{7}\right)$ and the values of table 6

4.6.6 YOBE

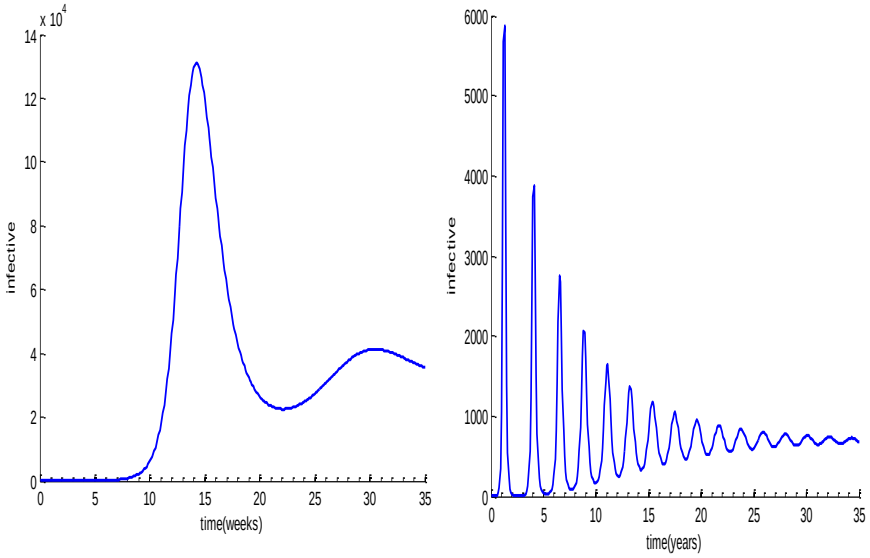

Figure 4.55 The epidemic curve for Yobe with N=2853828, $I_0 = 19\left(\frac{5}{7}\right)$ and the values of table 6

4.7 COMMENT ON SEIR (WITH VITAL DYNAMICS) SIMULATIONS

The characteristic exponential rise, turnover and decline (Earn, 2004) describing epidemic curves are evident in the numerical simulations of the SIR and SEIR (without vital dynamics) models examined. These models, while addressing the dynamics of an infectious disease albeit with the unique preference for a single epidemic episode are blind to the seemingly cyclic features observed in the incidence of measles in the regions as represented by figure 3.5. Introducing vital dynamics into the model rescued the simulations from the single epidemic scenario.

Figures (4.50 – 4.55) represent the simulation output of the attempt at this enterprise for the regions. Observe that there is a marked shift from the simulations generated in the previous sections. In the left pane (a weekly rendition) of the figures of this section, there is a second epidemic wave. This thus begins to capture the cyclic repetition highlighted in the discussion of

section 4.3. The right pane (a longer time scale) however gives an improved sustained cyclic repetition. The output of both time scales damps out as time evolved as opposed to a sustained un-damped oscillation noticed in the available data.

Given these considerations, the SEIR model with vital dynamics better represents the measles incidence data when compared with the earlier models examined.

4.8 SENSITIVITY ANALYSIS

Predictions or quantitative conclusions of a model are said to be sensitive to a parameter if a small change in the parameter causes a significant change in the outcome. A model is insensitive to a parameter if the outcomes are the same for a wide range of values of the parameter. Section 3.2.4 of qualitative analysis addressed the issue of some important parameters and established the threshold values of the parameters.

Sokoto is randomly chosen as the specimen region for the comparison of numerical simulations with the results obtained in the above mentioned section in the case of the basic reproduction number given that R_0 determines the size and duration of epidemics (Grais et al, 2006). Though not shown in this work, the result is equally true for the other regions studied.

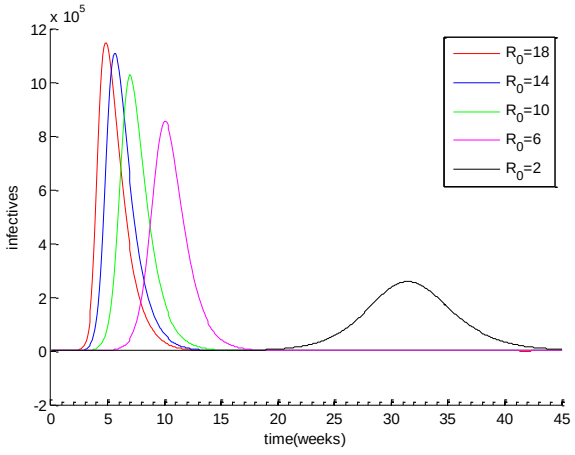

Figure 4.57 The epidemic curve for Sokoto with different values of $R_0 > 1$

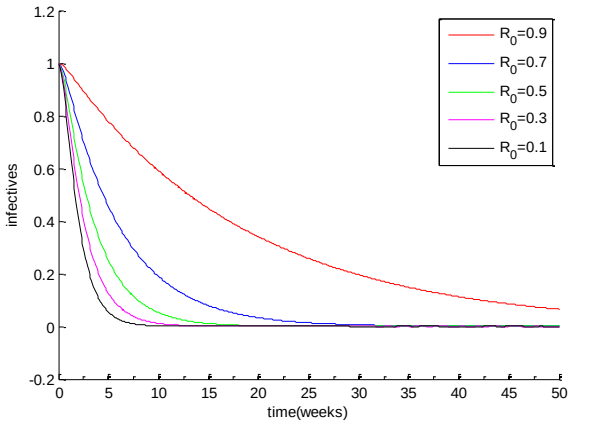

Figure 4.56 The epidemic curve for Sokoto with different values of $R_0 < 1$

It is observed from figure 4.57 that as R_0 decreases, the epidemic curve shifts to the right and its maxima reduces. This is insightful given that it shows it takes longer for the expected evolution of the disease in the population and the number of infective is significantly reduced. Thus reduced R_0 imparts positively in ameliorating the severity of the disease. Figure 4.56 shows that $\forall R_0 < 1$ the epidemic curve takes a downward turn as opposed to the expected exponential growth, thus, nullifying the possibility of an epidemic in the population. The results that there can be no epidemic if $R_0 < 1$ and there will be an epidemic if $R_0 > 1$ is thus numerically validated.

4.9 FOR FURTHER EXPLORATION

This work employed the Kermack – McKendrick SIR model and the SEIR model with and without vital dynamics to study the dynamics of measles in six regions representing the geopolitical zones of Nigeria. It assumed a constant contact rate. In the discussions of section 4.7, the output of the SEIR model with vital dynamics for both time scales damps out as time evolved as opposed to a sustained oscillation in the available data. This can be tied to the constant contact rate. Consequently, it is suggested that the dynamics be studied with a variable contact rate.

A non-constant population is closer home to the observed population dynamics given the continuous movement of people. Though, factoring this into the model will introduce more complexity, it is worth exploring.

Measles is predominantly a childhood disease though it is known to afflict adults that are not immunized. This study focused on ordinary differential equation models thus precluding age-related consideration. A partial differential equation (PDE) model affords the inclusion of age consideration. Thus, relevant data should be collected to facilitate an analysis with PDEs.

As pointed out (Grais et al, 2005; Keeling and Rohani, 2008 and Mostaco-Guidolin et al, 2009), the basic reproduction number is demographic sensitive although there is an established range for different infectious diseases. Region specific basic reproduction number and replacement number should be estimated using appropriate methods. This study did not engage in this exercise because it is beyond its scope. Reference (10 15 16 26 30 31 39) provide descriptions of different methods for their estimation.

4.10 CONCLUSION

The Kermack – McKendrick SIR model and the SEIR (with vital dynamics and without vital dynamics) models in relation to the Nigerian measles data were examined. Qualitative analysis allowed the exploration of the dynamics of the disease without explicitly solving the systems. Important parameters with threshold values helped determine under what condition an epidemic is possible. For a wholly susceptible population, this parameter is the basic reproduction number while the replacement number is the threshold parameter for a population that is not wholly susceptible.

The long term behavior of a dynamical system is of paramount biological importance. This behavior is known through the mechanism of stability analysis. This work established the necessary condition for the system to be stable.

Numerical simulations of the three models examined afforded the unique tool of exploring the significance of various parameters and parameter values and their interplay with the dynamics of measles. The significant difference between these simulations and the epidemiology data for the regions finds a plausible explanation in the notion of underreporting (Grais et al, 2006; Brauer, 2004) characteristic of epidemiological data.

Although very basic, the SIR model is insightful into the mechanism of the disease vis-à-vis the constituting compartments but handicapped in adequately describing the incidence of measles in the regions studied. A closer representation of the biology of the disease vis-à-vis its evolution is captured by the SEIR model. Although it is an improvement of the SIR model, it is inadequate in describing the measles incidence of the regions without vital dynamics.. As the study showed, the model with vital dynamics rescued the cyclic repetition highlighted in the discussion of section 4.3. Consequently, the SEIR model with vital dynamics is closest to the reality of the incidence data in spite of its inability to sustain the observed oscillations.

Some practical implications can be drawn from the fore-going analysis in reducing and/or eradicating measles incidence from the population. From the analysis of section 3.2.4, the necessary condition for measles to fizzle out of the population is $R_0 < 1$ for a wholly susceptible population or $R < 1$ for a population not wholly susceptible. Focus will be on the latter as it indicates the severity with which the epidemic grows. To force the effective reproduction number below the threshold value of one, the following considerations hold. Recall that $R = \frac{r}{a} S_0$

- The rate of infection (r) of the susceptible class per unit time should be reduced. Militating against contacts with the infective by way of quarantining the infective is a good practice. Given the modes of infection by the measles virus, being more attentive to hygiene by way of washing hands upon touching surfaces that may be contaminated and avoiding crowded places reduces the risk and rate of infection.
- Reducing the number of susceptible in the population is of significant importance. This is done readily by increasing the number of those who are immune by way of vaccination. As pointed out by Murray (2002), mass vaccination is the cheapest and most effective means of

disease control. The reality of vaccination against measles in Nigeria is not as high as one would expect it given that "the current national measles vaccination coverage is 62% with a very wide variation in the country that has once achieved coverage of 80% with routine immunization" Adeboye et al (2011). The authors' work, while not sufficient to form a basis for the generalization (given that it was carried out in Bida, Niger State only) is indicative of its possibility and perhaps its likelihood.

REFERENCES

1. Adeboye, M., Adesiyun, O., Adegboye, A., Eze, E., Abubakar, U., Ahmed, G., Usman, A., Amos, S., and BF Rotimi, B.F. (2011). Measles in a Tertiary Institution in Bida, Niger State, Nigeria: Prevalence, Immunization Status and Mortality Pattern. *Oman Medical Journal* 26(2), 114-117

2. Anderson, R.M. and May, R.M. (1982). Directly Transmitted Infectious Diseases: Control by Vaccination. *Science*, 215 (4536), 1053 – 1060.

3. Apostolou, M. (2011). *Numerical algorithms and mathematics for ODE models of measles* MPhil Thesis, University of Portsmouth. Accessed on 25/01/2013 from http://eprints.port.ac.uk

4. Asor, V.E. and Ugwu, C. (2011). A new mathematical model to simulate infectious disease dynamics in Rivers State, Nigeria. *International Journal of Computer Science Issues*, 8(2), 290 – 295.

5. Axton, J.H.M. (1979). The Natural History of Measles. *Journal of the University of Zimbabwe,* 7(2), 139 – 154. Accessed on 09/01/2013 from http://archive.lib.msu.edu/DMC/African%20Journals/pdfs/Journal%20of%20the%20 University%20of%20Zimbabwe/vol7n2/juz007002003.pdf

6. Bakare, E.A., Adekunle, Y.A., and Kadiri, K.O. (2012). Modeling and simulation of the dynamics of the transmission of measles. *International Journal of Computer Trends and Technology*, 3(1), 174 – 178

7. Bradsher, C.A., Stotts, R.C., Carter, M.A., and Grabowsky, M. (2006). The measles initiative to control measles in Kenya. *Public Health Nursing*, 24(1), 26 – 33.

8. Brauer, F. (2004). What does mathematics have to do with SARS? *Pi in the sky*, (8), 10 – 13.

9. Brauer, F. (2006). Some simple epidemic models. *Mathematical Biosciences and Engineering*, 3(1), 1 – 15

10. Cintron-Arias, A., Castillo-Chavez, C., Bettencourt, L.M.A., Lloyd, A.L., and Banks, H.T. (2009). The estimation of the effective reproductive number from disease outbreak data. *Mathematical Biosciences and Engineering*, 6(2), 261 – 282.

11. Earn, D.J.D. (2004). Mathematical modeling of recurrent epidemics. *Pi in the sky*, (8), 14 - 17.

12. Edelstein-Keshet, L. (2005). *Mathematical models in biology* Society for Industrial and Applied Mathematics. Philadelphia

13. Fraser, C., and Grassly, N.C. (2008). Mathematical models of infectious disease transmission. *Nature Reviews Microbiology*, 6(6), 477 – 487.

14. Glenn, L. (2005). *Differential equations: a modeling approach.* McGraw-Hill NY10020

15. Grais, R.F., Ferrari, M.J., Dubray C., Bjørnstad, O.N., Grenfell, B.T., Djibo A., Fermon F., and Guerin, P.J. (2006). Estimating transmission intensity for a measles epidemic in Niamey, Niger: lessons for intervention. *Transactions of the Royal Society of Tropical Medicine and Hygiene* 100, 867—873.

16. Heffernan, J.M., Smith, R.J., and Wahl, L.M. (2005). Perspectives on the basic reproduction ratio. *Journal of the Royal Society Interface*, 2, 281 – 293.

17. Hethcote, H.W. (1989). Three basic epidemiological models, in *Applied Mathematical Ecology*, Gross, L., Hallam, T.G., and Levin, S.A., (Eds). Springer - Verlag, Berlin. 119 – 144

18. Hethcote, H.W. (2005). *The basic epidemiology models I & II: models, expressions for R_o, parameter estimation and applications.* Institute for Mathematical Sciences, National University of Singapore

19. Hirsch, M.W., Smale, S. and Devaney R.L. (2003). *Differential equations, dynamical systems and an introduction to chaos* (2nd edition). Academic Press.

20. Hirst, E., William, L. and Cope, J. (1977). Simulation model of household fuel uses. *Applied Mathematical Modeling*, 1, 177 – 180.

21. Jordan, D.W. and Smith, P. (2007). *Nonlinear ordinary differential equations: An introduction for scientists and engineers* 4th edition. Oxford University Press

22. Keeling, M.J. and Rohani, P. (2008). *Modeling infectious diseases in humans and animals.* Princeton University Press. Princeton and Oxford.

23. Klemens, B. (2009). *Modeling with data: tools and techniques for scientific computing.* Princeton University Press. Princeton and Oxford.

24. Koriko, O. and Yusuf, T.T. (2008). Mathematical model to simulate tuberculosis disease population dynamics. *American Journal of Applied Sciences,* 5(4), 301 – 306.

25. Lewis, M. (2004). Mathematical models and Infectious disease dynamics. *Pi in the sky* (8), 4.

26. Lloyd A.L and May R.M. (1996). Spatial Heterogeneity in Epidemic Models. *Journal of theoretical biology* 179 (1), 1 – 11.

27. Macdonald, B., Shakarian P. and Moores, G. (2012). *Spreaders in the network SIR model: An empirical study.* Accessed on 10/02/2013 from http://arxiv.org/pdf/1208.4269v2.pdf

28. McLean, A.R and Anderson, R.M. (1988). Measles in developing countries Part 1. Epidemiological parameters and patterns. *Epidemiology and Infection,* 100 (1), 111 – 133.

29. Mathews, J.H., and Fink, K.D. (2004). *Numerical methods using Matlab* (4th edition). Pearson Education Inc. N.J

30. Mostaço-Guidolin, L.C., Greer, A., Sander, B., Wu, J., and Moghadas, S.M. (2011). Variability in transmissibility of the 2009 H1N1pandemic in Canadian communities. *BMC Research Notes*, 4, 537.

31. Mostaço-Guidolin, L.C., Bowman, C.S., Greer, A.L., et al. (2012). Transmissibility of the 2009H1N1 pandemic in remote and isolated Canadian communities: a modelling study. BMJ Open 2012;2:e001614. doi:10.1136/bmjopen-2012-001614

32. Miller K. (2003). *Encyclopedia and Dictionary of Medicine, Nursing and Allied Health* (7th edition). Saunders, Elsevier Inc.

33. Murray, J. D. (2002). *Mathematical Biology: An introduction* (3rd edition). Springer-Verlag, Berlin

34. Otto, S.R. and Denier, J.P. (2005). *An Introduction to Programming and Numerical Methods in Matlab.* Springer-Verlag. London

35. Rodriguez-Mesa, A.M. (2012). *Spatial and temporal dynamics of infected populations: the Mexican epidemic.* Accessed on 10/02/2013 from http://arxiv.org/pdf/1204.2761.pdf

36. Shampine, L. F., and Reichelt, M.W. (1997). The matlab ode suite. *SIAM Journal on Scientific Computing*, 18, 1 – 22.

37. Teschl, G. (2012). *Ordinary Differential Equations and Dynamical Systems.* American Mathematical Society. Providence, Rhode Island

38. Trottier, H. and Philippe, P. (2002). Deterministic modeling of infectious diseases: Applications to measles and other similar infections. *The internet journal of infectious diseases*, 2(1). Accessed on 19/05/2013 http://dx.doi.org/10.5580/89b

39. Varah, J.M. (1982). *A computational approach to parameter estimation in ordinary differential equations*. University of Waterloo. CS–82–58. Accessed on 03/07/2013 from https://cs.uwaterloo.ca/research/tr/1982/CS-82-58.pdf

40. Center for Disease Control (CDC) http://www.cdc.gov/measles/about/overview.html Accessed on 22/01/2013

41. Center for Disease Control (CDC) http://www.cdc.gov/vaccines/pubs/pinkbook/downloads/meas.pdf Accessed on 20/05/2013

42. WHO. http://www.who.int/mediacentre/factsheets/fs286/en Accessed on 20/05/2013

43. WHO. http://apps.who.int/gho/data/node.main.688?lang=en accessed on 20/05/2013

LIST OF TABLES

LIST OF FIGURES

APPENDIX A

The map was downloaded on 01/07/2013 from
http://collections.infocollections.org/whocountry/index/assoc/s7928e/p08.jpg

APPENDIX B

S/N	State	Zone	Cases
1	Abia	South - East	95
2	Anambra		180
3	Ebonyi		69
4	Imo		222
5	Enugu		108
Zonal Sub - Total			**674**
6	Akwa Ibom	South - South	102
7	Bayelsa		86
8	Cross River		79
9	Delta		177
10	Edo		138
11	Rivers		51
Zonal Sub - Total			**633**
12	Ekiti	South - West	241
13	Lagos		352
14	Ogun		244
15	Ondo		29
16	Osun		74
17	Oyo		162
Zonal Sub - Total			**1102**

S/N	State	Zone	Cases
18	Adamawa	North - East	181
19	Bauchi		24
20	Borno		155
21	Gombe		114
22	Taraba		464
23	Yobe		653
Zonal Sub – total			**1591**
24	Benue	North - Central	355
25	FCT		84
26	Kogi		266
27	Kwara		85
28	Nasarawa		148
29	Niger		285
30	Plateau		142
Zonal Sub – total			**1365**
31	Jigawa	North - West	144
32	Kaduna		757
33	Kano		152
34	Katsina		231
35	Kebbi		1985
36	Sokoto		2332
37	Zamfara		95
Zonal Sub – total			**5696**

Nigeria zonal measles incidence data (2012)
The data is available from IDSR 003 database from the Surveillance Branch, Epidemiology Division, Nigeria Center for Disease Control, Federal Ministry of Health, Abuja.

Week	Benue	Delta	Imo	Lagos	Sokoto	Yobe
5	9	4	2	7	34	19
6	37	1	3	9	76	6
7	2	3	0	12	43	33
8	44	3	19	21	85	23
9	16	14	10	0	162	15
10	44	3	6	9	222	8
11	15	3	3	17	186	11
12	16	4	3	22	148	15
13	11	6	2	12	133	46
14	1	2	16	10	77	38
15	1	5	5	10	141	28
16	7	4	0	5	49	30
17	16	3	6	13	38	27
18	1	5	0	12	132	19
19	16	5	6	13	27	30
20	9	2	2	10	50	44
21	3	2	5	5	165	37
22	4	5	0	8	62	25
23	0	4	6	4	26	34
24	0	6	12	6	11	30
25	2	3	6	0	18	19
26	5	2	2	8	6	16
27	11	0	2	0	13	8
28	7	2	6	0	0	10
29	0	1	6	5	3	4
30	6	3	2	9	0	8
31	18	5	1	12	0	9
32	9	4	1	5	18	5
33	0	2	4	18	0	4
34	3	3	5	8	30	4
35	2	6	4	4	4	10

The weekly measles incidence data for the 6 regions under study

Year	Nigeria
1980	162106
1981	129671
1982	139785
1983	136778
1984	182591
1985	161768
1986	115743
1987	77566
1988	75908
1989	33678
1990	115682
1991	44026
1992	85965
1993	54734
1994	106081
1995	12393
1996	88675
1997	21385
1998	143098
1999	217151
2000	212183
2001	168107
2002	42007
2003	141258
2004	31521
2005	110927
2006	704
2007	2613
2008	9960
2009	1272
2010	8491
2011	18843

Nigeria annual measles incidence (1980 – 2011).